Table 3 Effect of amputation of the uterine corpus immediately following cesarean delivery

Subjects	CRH with amputation $n = 3$	CRH without amputation $n = 2$	RH $n = 209$	p value*
Age	30.3 (24–37)**	34.5 (32–37)	48.4 (18–75)	0.37
Op. time (mins)	186.0 (160–228)**	412.5 (400–425)	297.3 (147–645)	0.043
EBL (ml)	1034.3 (730–1540)	3715.0 (3280–4150)+	858.8 (150–4770)	0.043
Transfusion	0	2 (100%)	106 (50.7%)	0.046

Mean with range or mean with percentage is shown. Nonparametric Wilcoxon signed-rank test or the Mann–Whitney U test was used for the statistical analysis

CRH with amputation cesarean radical hysterectomy with amputation of the uterine corpus, *CRH without amputation* cesarean radical hysterectomy without amputation of the uterine corpus, *RH* radical hysterectomy, *EBL* estimated blood loss

* p values for the statistical evaluation were between CRH with amputation and CRH without amputation; ** $p < 0.05$, CRH with amputation versus RH; + $p = 0.017$, CRH without amputation versus RH

[2]. In our study, the prevalence of cervical cancer complicating pregnancy was 2.3%; a similar proportion to that already reported. This indicates to clinicians that cervical cancer is not rare in pregnancy.

For nonpregnant women, the standard surgical approach to Stage IB and IIA cervical cancer consists of a RH [3]. The management of pregnant patients with early-stage cervical cancer is similar to that of nonpregnant patients, and radical surgery is one of the treatment options [2]. Because there is a high recurrence rate of cervical cancer in those patients who deliver vaginally (10 out of 17), Sood et al. [4] recommend cesarean section as the mode of delivery for pregnant women with cervical cancer.

It is reported that the serious complication rate in CRH is lower than that of radiation therapy (6.7 vs. 28.8%) [6]. However, compared to RH for nonpregnant women, heavier blood loss during surgery (1750 vs. 777 ml) and a higher transfusion rate (75 vs. 54%) were also reported [7]. Duggan et al. [8] reported a median EBL during CRH of 1300 ml (range 250–5250), with 37.5% needing blood transfusion during surgery. Heavy blood loss is a potential major complication of CRH.

Although our study is limited by the number of subjects, similar results are seen in our study (Table 1): the blood loss for the CRH group was more than twice that of the nonpregnant RH group (mean, 2106.6 vs. 858.8 ml, $p < 0.001$). Major blood loss (over 2000 ml) was seen in two out of five cases (40%) in the CRH group, while it was seen in 19 out of 209 cases (9.1%) in the nonpregnant RH group. Thus, any surgical modifications made in an attempt to reduce the blood loss in CRH are valuable, although literature addressing the surgical procedure for RH is limited [10].

Removing the uterine corpus following cesarean section is defined as the amputation of uterine corpus in our project. Compared to the nonpregnant uterus, the gravid uterus, especially in the late stage of pregnancy, is remarkably enlarged and thus disturbs the surgical field, making surgery difficult. The pregnant uterus could also be the source of atonic bleeding. As seen in one of the CRH cases without amputation of the uterine corpus, covering the surgical cloth meant that the surgeons did not realize that significant bleeding from the uterus passed through the vagina. Pregnant uterine corpus could be the source of heavy blood loss. By removing the uterine corpus after the ligation of the uterine arteries following cesarean delivery, this source of bleeding could be eliminated, making surgery less complicated (Table 3). Mean EBL and operating time for CRH with amputation of the uterine corpus were both far less than in the cases where amputation of uterine corpus was not performed: EBL, 1034.3 ml (730–1540) versus 3715.0 ml (3280–4150), $p < 0.043$; operating time, 186.0 min (160–228) versus 412.5 min (400–425), $p < 0.043$. These significant differences tell us that intraoperative amputation of the uterine corpus may be recommended as the standard surgical procedure for the CRH.

Our data show a significantly younger age at diagnosis for cervical cancer during pregnancy compared to nonpregnant cervical cancer subjects (32.0 years of age vs. 48.4 years of age, $p < 0.001$), which was similar to the previously reported data (34.0 ± 5.9 years) [11]. The prognosis of early-stage cervical cancer in pregnant women is similar to that of nonpregnant patients when standard treatment is given [12]. There was no overall difference in survival rate in young cervical cancer patients compared to older patients [13]. Thus, CRH with less blood loss will positively impact the patient's care, reducing the risk of intra- or postoperative morbidity and mortality, including the need for transfusion, thereby decreasing the risk of transfusion-related adverse effects such as hepatitis or HIV infection. As our data show, the risk of transfusion is decreased by performing amputation of the uterine corpus in cervical hysterectomy (Table 3). Since it not only reduces the risk of surgical complication, but also reduces the prevalence of transfusion, amputation of the uterine corpus may be considered as the standard surgical procedure during CRH.

Because there are no previously reported data, we do not know if amputation of the uterine corpus during CRH increases the risk of intraoperative tumor exposure to the peritoneum cavity. Among the three planned amputation cases, there were no intraoperative tumor exposure cases. With follow-ups ranging from 8 to 48 months, there were no cases of local or peritoneal recurrence, although there was one case of distant metastasis to Virchow's lymph nodes for the subject who underwent amputation of the uterine corpus during CRH. Surgeons must be aware of the possibility of intraoperative tumor exposure whenever amputation of the uterine corpus is performed during CRH.

The strength of our study is that we firstly demonstrated the possible utility of amputation of the uterine corpus during CRH to minimize the risk of surgery. The weakness of the study is that this is a retrospective study that may miss confounding factors. For example, although planned amputation of the uterine corpus was seen in three cases of CRH, there was no documentation regarding how and when they selected these cases. We were also unable to obtain the indication for RH among cases with Stage IA. Possible confounding factors affecting the performance of RH, such as patient body habitus or surgeon's level of training/career as gynecologic oncologist should also be considered.

Our study was limited in terms of the number of subjects undergoing CRH. In order to evaluate the efficacy of amputation of the uterine corpus during CRH, further investigation with a larger number of subjects is mandatory.

Conflict of interest statement No author has any conflict of interest.

References

1. Tewari K, Cappuccini F, Gambino A et al (1998) Neoadjuvant chemotherapy in the treatment of locally advanced cervical carcinoma in pregnancy. Cancer 82:1529–1534
2. Nguyen C, Montz FJ, Bristow RE (2000) Management of stage I cervical cancer in pregnancy. Obstet Gynecol Surv 55:633–643
3. Donato DM (1999) Surgical management of stage IB–IIA cervical carcinoma. Semin Surg Oncol 16:232–235
4. Sood AK, Sorosky JI, Mayr N et al (2000) Cervical cancer diagnosed shortly after pregnancy: prognostic variables and delivery routes. Obstet Gynecol 95:832–838
5. Brunschwig A, Barber HR (1958) Cesarean section immediately followed by radical hysterectomy and pelvic node excision. Am J Obstet Gynecol 76:199–203
6. Nisker JA, Shubat M (1983) Stage IB cervical carcinoma and pregnancy: report of 49 cases. Am J Obstet Gynecol 145:203–206
7. Monk BJ, Montz FJ (1992) Invasive cervical cancer complicating intrauterine pregnancy: treatment with radical hysterectomy. Obstet Gynecol 80:199–203
8. Duggan B, Muderspach LI, Roman LD et al (1993) Cervical cancer in pregnancy: reporting on planned delay in therapy. Obstet Gynecol 82:598–602
9. Rock JA, Thompson JD et al (1997) Te Linde's operative gynecology, 8th edn. Lippincott-Raven, Philadelphia, pp 771–883
10. Magrina JF, Goodrich MA, Weaver AL et al (1995) Modified radical hysterectomy: morbidity and mortality. Gynecol Oncol 59:277–282
11. Antonelli NM, Dotters DJ, Katz VL et al (1996) Cancer in pregnancy: a review of the literature. Obstet Gynecol Surv 51:125–134
12. van der Vange N, Weverling GJ, Ketting BW et al (1995) The prognosis of cervical cancer associated with pregnancy: a matched cohort study. Obstet Gynecol 85:1022–1026
13. Brewster WR, DiSaia PJ, Monk BJ et al (1999) Young age as a prognostic factor in cervical cancer: results of a population-based study. Am J Obstet Gynecol 180:1464–1467

Jpn J Radiol (2010) 28:95–100
DOI 10.1007/s11604-009-0387-3

ORIGINAL ARTICLE

Diagnostic performance of fluorodeoxyglucose positron emission tomography/magnetic resonance imaging fusion images of gynecological malignant tumors: comparison with positron emission tomography/computed tomography

Kazuya Nakajo · Mitsuaki Tatsumi · Atsuo Inoue
Kayako Isohashi · Ichiro Higuchi · Hiroki Kato
Masao Imaizumi · Takayuki Enomoto
Eku Shimosegawa · Tadashi Kimura · Jun Hatazawa

Received: July 29, 2009 / Accepted: September 28, 2009

Abstract
Purpose. We compared the diagnostic accuracy of fluorodeoxyglucose positron emission tomography/computed tomography (FDG PET/CT) and PET/magnetic resonance imaging (MRI) fusion images for gynecological malignancies.
Materials and methods. A total of 31 patients with gynecological malignancies were enrolled. FDG-PET images were fused to CT, T1- and T2-weighted images (T1WI, T2WI). PET-MRI fusion was performed semiautomatically. We performed three types of evaluation to demonstrate the usefulness of PET/MRI fusion images in comparison with that of inline PET/CT as follows: depiction of the uterus and the ovarian lesions on CT or MRI mapping images (first evaluation); additional information for lesion localization with PET and mapping images (second evaluation); and the image quality of fusion on interpretation (third evaluation).
Results. For the first evaluation, the score for T2WI (4.68 ± 0.65) was significantly higher than that for CT (3.54 ± 1.02) or T1WI (3.71 ± 0.97) ($P < 0.01$). For the second evaluation, the scores for the localization of FDG accumulation showing that T2WI (2.74 ± 0.57) provided significantly more additional information for the identification of anatomical sites of FDG accumulation than did CT (2.06 ± 0.68) or T1WI (2.23 ± 0.61) ($P < 0.01$). For the third evaluation, the three-point rating scale for the patient group as a whole demonstrated that PET/T2WI (2.72 ± 0.54) localized the lesion significantly more convincingly than PET/CT (2.23 ± 0.50) or PET/T1WI (2.29 ± 0.53) ($P < 0.01$). Conclusion. PET/T2WI fusion images are superior for the detection and localization of gynecological malignancies.

Key words PET · MRI · Fusion image · Gynecological malignant tumors

K. Nakajo · M. Tatsumi · A. Inoue · K. Isohashi · I. Higuchi · H. Kato · M. Imaizumi · E. Shimosegawa · J. Hatazawa (✉)
Department of Nuclear Medicine and Tracer Kinetics, Osaka University Graduate School of Medicine, 2-2 Yamadaoka, Suita 565-0871, Japan
Tel. +81-6-6879-3461; Fax +81-6-6879-3469
e-mail: kazuyan@tracer.med.osaka-u.ac.jp

J. Hatazawa
Department of Radiology, Osaka University Hospital, Suita, Japan

T. Enomoto · T. Kimura
Department of Obstetrics and Gynaecology, Osaka University Graduate School of Medicine, Suita, Japan

Introduction

Inline positron emission tomography/computed tomography (PET/CT) systems provide highly accurate fusion images of metabolic and anatomical images that are useful for detecting malignant tumors and their locations.[1,2] However, contrast resolution of CT for different tissues is limited especially in the head and neck and pelvis when low-dose exposure is employed. In contrast, magnetic resonance imaging (MRI) has several advantages over CT, such as high tissue contrast and no radiation exposure. The diagnostic ability of MRI for uterine cervical carcinoma and ovarian masses was proven to be higher than that of CT owing to the high tissue contrast of the former.[3–5] In the study presented here, we exam-

ined the usefulness of PET/MR fusion images in comparison with that of inline PET/CT for evaluating gynecological tumors. We hypothesized that PET/T2WI was superior to other fusion images, such as PET/CT, for gynecological tumors.

Materials and method

Patients

From April 2007 to May 2008, a total of 31 patients with gynecological cancer were retrospectively analyzed by means of inline PET/CT with 2-deoxy-2-[^{18}F]fluoro-D-glucose (FDG) and by MRI within a month. The clinical information is summarized in Table 1. There were 25 patients with uterine cervical cancer, 3 with endometrial cancer, and 3 with ovarian cancer. In all, 21 of the 25 patients were studied before undergoing any treatment, and the others were studied after surgical resection, radiotherapy, chemotherapy, or radiochemotherapy.

PET/CT scanning

All of the patients were fasted at least 4 h before injection of FDG at a dose of 3.7 MBq/kg. After intravenous administration, patients were asked to remain still in a dark, quiet room for 60 min. Whole-body PET imaging was started immediately after CT imaging at 60 min after injection (Gemini GXL; Philips Medical Systems, Eindhoven, The Netherlands). Acquisition parameters for the CT portion (16-slice CT) consisted of breath-holding during normal expiration, scanning from the level of the apex to the lower pole of the pelvis, no intravenous or oral contrast media, 120 kVp and 50 effective mAs, and 5.0 mm slice thickness/4.0-mm interval. The PET images were acquired with the following parameters: three-dimensional (3D) emission scan, 2 min scan/bed position × 11 positions (15 cm/position), ordered-subset expectation maximization (OSEM) reconstruction, 4.0 mm slice thickness/interval.

Table 1. Patients' characteristics

Total no. of patients	31
Median age (years)	57.6 (range 34–85)
Median tumor size (mm)	43.7 (range 10.0–166.7)
Diagnoses of gynecological malignant lesions	
Cervical cancer	25
Endometrial cancer	3
Ovarian cancer	3
History of treatment	
Cervical cancer	
None	18
CT	0
RT	2
CRT	2
Operation	1
Endometrial cancer	1
None	
CT	1
RT	1
Ovarian cancer	2
CT + operation	1

CT, chemotherapy; RT, radiotherapy; CRT, chemoradiotherapy

MRI scanning

The MRI study was performed with a 1.5 T MRI system (Signa Excite HD 1.5T; GE Medical Systems, Waukesha, WI, USA) or a 3.0 T MRI system (Signa Excite HD 3.0T; GE Medical Systems) within 1 month before or after PET/CT imaging. We used non-contrast-enhanced transaxial T1-weighted images (T1WI) and T2-weighted images (T2WI) for image fusion. The T1WI were acquired with a 3D spoiled gradient recalled echo (GRE) sequence using the fat-suppression technique. The respective imaging parameters of the 1.5 T and 3.0 T scanners were TR 5.1 and 4.7 ms, TE 2.4 and 4.2 ms; flip angle 12° and 12°; slice thickness 3.0 and 4.0 mm (no gap). The T2WI were obtained with a single-shot fast spin echo (FSE) sequence using the following parameters for both 1.5-T and 3.0-T scanners: TR 6000 ms, TE 80 ms, 5.0 mm slice thickness/1-mm interslice gap.

Image fusion

The PET and MRI image fusion was semiautomatically done using Osirix imaging software (version 3.2.1).[6] Osirix uses ITK (Insight Segmentation and Registration Toolkit) which employs leading-edge segmentation and registration algorithms in two, three, and more dimensions. First, we selected transaxial images of the CT scans of PET/CT and MRI T2WI corresponding to the femoral head in each patient by visual inspection. Second, 3D space adjustments were applied to both PET/CT and MRI T1WI and T2WI. The PET images were fused on the MRI images for image analysis.

Image analysis

Two nuclear medicine physicians inspected images having the information that the patients have gynecological cancer. They visually inspected CT, noncontrast T1WI, T2WI, PET/CT, PET/T1WI, and PET/T2WI scans of gynecological malignancies. They evaluated the depiction of lesions by CT, T1WI, and T2WI, as well as the localization of abnormal FDG uptake, by means of side-by-side inspection of PET and CT (PET+CT), PET

and T1WI (PET+T1WI), and PET and T2WI (PET+T2WI) according to the rating scale described below. The final evaluation was of how convincingly the abnormal accumulations in certain lesions were diagnosed using PET/CT, PET/T1WI, and PET/T2WI. The rate of agreement for the two physicians was also assessed for each evaluation. In case of disagreement, consensus evaluation was obtained after discussion.

First, the depiction of the primary tumor in the uterus and ovarian malignancy on CT images, T1WI, and T2WI was evaluated with the following five-point rating scale 1, definitely no lesions; 2, probably no lesions; 3, equivocal finding; 4, probably positive lesions; 5, definitely positive lesions. Second, we placed PET images side by side with CT images, T1WI, and T2WI (PET+CT, PET+T1WI, and PET+T2WI, respectively) for evaluation of how much additional information for lesion localization was provided by CT, T1WI, and T2WI. For this evaluation a three-point rating scale was used: 1, no additional information was provided regarding the site of FDG accumulation; 2, the site of the FDG accumulation was possibly localized; 3, the site of the FDG accumulation was definitely identified.

Third, we assessed the quality of diagnosis by PET/CT, PET/T1WI, and T2WI in terms of how convincingly FDG accumulation was detected in certain anatomical structures. For this assessment, the following three-point rating scale was used: 1, poor; 2, acceptable; 3, excellent. The analysis was performed for the patient group as a whole and for patient subgroups classified according to the magnitude of FDG accumulation. The FDG accumulation was evaluated in terms of maximum standardized uptake value (SUV_{max}) in the region of interest (ROI). The threshold for accumulation was set at 3.0 of SUV_{max}, and the patients were divided into two subgroups: those with $SUV_{max} \geq 3.0$ ($n = 25$) and those with $SUV_{max} < 3.0$ ($n = 6$).

Statistics

The five-point rating scale for lesion detection by CT, T1WI, and T2WI and the three-point rating scale for fusion images were statistically analyzed with the Wilcoxon matched-pair signed-rank test. The rate of agreement between the two physicians was assessed using a weighted kappa coefficient, which was statistically compared by means of Student's *t*-test.

Results

For the first evaluation—depiction of the uterus and the ovarian lesions on CT images, T1WI, and T2WI—the kappa coefficients of agreement between the two physicians were 0.70 ± 0.103 for CT, 0.70 ± 0.09 for T1WI, and 0.80 ± 0.07 for T2WI. The rate of agreement was significantly higher for T2WI than for CT ($P < 0.05$) or T1WI ($P < 0.05$). After consensus was reached about lesion detection, the scores for lesion detection by CT, T1WI, and T2WI were 3.54 ± 1.02, 3.71 ± 0.97, and 4.68 ± 0.65, respectively. The score for T2WI was significantly higher than those for CT or T1WI ($P < 0.01$).

For the second evaluation—how much additional information for lesion localization was provided by CT, T1WI, and T2WI—the rates of agreement between the two physicians were 0.62 ± 0.24 for PET+CT, 0.54 ± 0.14 for PET+T1WI, and 0.66 ± 0.11 for PET+T2WI. There was no significant difference in the rate of agreement among these methods. The scores for the localization of FDG accumulation by PET+CT, PET+T1WI, and PET+T2WI were 2.06 ± 0.68, 2.23 ± 0.61, and 2.74 ± 0.57, respectively, which indicated that T2WI provided significantly more additional information for the identification of anatomical sites of FDG accumulation than did CT ($P < 0.01$).

For the third evaluation—the quality of diagnosis by PET/CT, PET/T1WI, and T2WI—the rates of agreement between the two physicians were 0.64 ± 0.130 for PET/CT, 0.59 ± 0.129 for PET/T1WI fusion images, and 0.79 ± 0.12 for PET/T2WI fusion images. The rate of agreement was significantly higher for PET/T2WI than for PET/CT or PET/T1WI ($P < 0.05$). After consensus was reached, the three-point rating scale for the patient group as a whole demonstrated that PET/T2WI (2.72 ± 0.542) localized the lesion significantly more convincingly than PET/CT (2.23 ± 0.50) or PET/T1WI (2.29 ± 0.53) ($P < 0.01$).

In the subgroup analysis, the scores on the three-point rating scale for patients with SUV_{max} of ≥3.0 ($n = 25$) were 2.32 ± 0.476 for PET/CT, 2.40 ± 0.500 for PET/T1WI, and 2.72 ± 0.541 for PET/T2WI. The corresponding scores for patients with SUV_{max} of <3.0 ($n = 6$) were 1.83 ± 0.408, 1.83 ± 0.408, and 2.67 ± 0.516, respectively. The rating scale between the subgroups showed a significant reduction for PET/CT ($P < 0.01$) and PET/T1WI ($P < 0.01$) but not for PET/T2WI (Figs. 1, 2).

Discussion

T2WI is superior to CT in its ability to detect lesions of uterine and ovarian cancer.[1–5] T2WI, even with low-magnetic-field MRI, has proven itself superior for staging uterine carcinoma,[7,8] and it was found to be able to depict an intramural nodule and abnormal wall thickening, which indicate a malignant lesion.[3,5] The results of

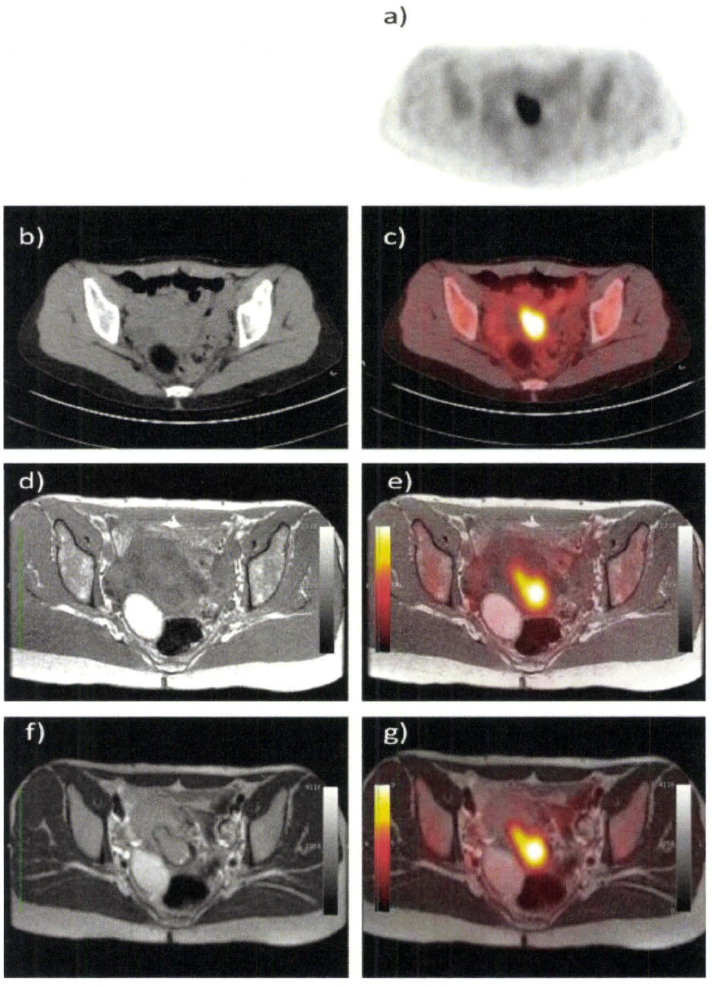

Fig. 1. Case of cervical cancer. Positron emission tomography (PET) shows abnormal accumulation of fluorodeoxyglucose (FDG) in the pelvis. The lesion is not clear on the computed tomography (CT) scan with magnetic resonance T1-weighted imaging (T1WI), whereas the uterine cervix shows a mass lesion with T2WI. With fusion imaging, the lesion seen with T2WI accords with an abnormal accumulation of FDG. **a** CT. **b** CT/PET fusion. **c** T1WI. **d** T1WI/PET fusion. **e** T2WI. **f** T2WI/PET fusion

our analyses of CT obtained with the PET/CT system and MRI were consistent with those of previous studies,[9,10] which is the result of the high tissue contrast provided by T2WI.

Localization of the site of FDG accumulation is important for FDG-PET imaging. When mass lesions depicted by CT or MRI are associated with FDG accumulation, they are diagnosed as metabolically active and with a high probability of malignancy. PET/CT and PET/MRI fusion images are therefore especially beneficial for diagnosing lymph node metastasis.[11–13]

Differentiation of physiological from abnormal FDG accumulation is also important on FDG-PET diagnosis. SUV_{max} of 3.0 has been used as a differentiation index.[14–16] In the pelvis, FDG is known to accumulate in the normal uterine endometrium, ovary, urinary tract, rectum, and colon. The magnitude of physiological FDG accumulation varies as the urinary tract may have an SUV_{max} of more than 10.0 or endometrium may have an SUV_{max} of <3.0.[15] The SUV_{max} value itself is therefore not a reliable index. Instead, when FDG accumulation is found in normal organs or tissues as confirmed by CT or MRI, a convincing diagnosis of physiological accumulation can be made.

Our study demonstrated that the site of FDG accumulation can be more accurately identified by T2WI than by CT or T1WI. It is therefore only reasonable that PET/T2WI fusion images produced a more convincing diagnosis of the anatomical site of FDG accumulation than did CT or T1WI.[3] It is noteworthy that the ability to localize low-level FDG accumulation significantly deteriorated when CT or T1WI was utilized for fusion images. In several patients, mild to moderate FDG accumulation was found in small masses depicted by T2WI but not by CT or T1WI. FDG accumulation fused on the T2WI was correctly evaluated in these patients after taking the partial volume effect into account.

Our study indicated that separately obtained but fused PET/T2WI images are superior to the PET/CT images obtained with inline PET/CT. This is partly due

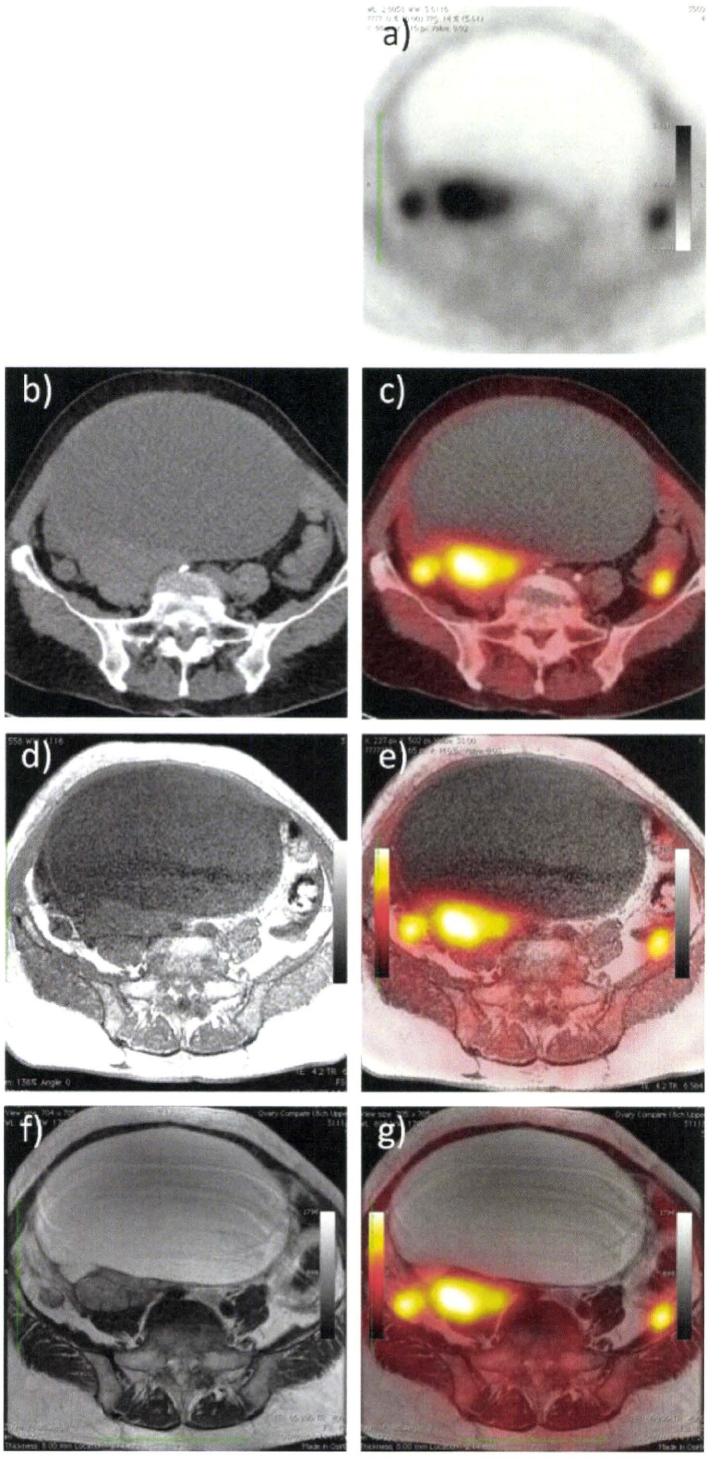

Fig. 2. Case of ovarian serous cystadenocarcinoma. PET shows abnormal accumulation in the pelvis. With CT and MRI T1WI, the border of a solid portion and the cystic ingredient is indistinct. With T2WI, the border of a solid portion and the cystic portion becomes clear. Also, with the fusion image, we confirm a solid portion and show abnormal accumulation of FDG. **a** CT. **b** CT/PET fusion. **c** T1WI. **d** T1WI/PET fusion. **e** T2WI. **f** T2WI/PET fusion

to the fact that the CT images of PET/CT were obtained with limited radiation exposure whereas the MRI images were obtained with high-quality MRI systems, so the diagnostic ability of PET/CT fusion images was partly underestimated.

Several trials have reported improved diagnostic ability of PET/CT for uterine cancer and ovarian cancer.[17–19] Kitajima et al. employed contrast-enhanced CT in addition to FDG PET/CT, and anatomical information on abnormal FDG accumulation was much

improved by fusing FDG PET images with those of the contrast-enhanced CT.[18,19]

A drawback of the PET/MRI fusion images is misregistration due to the movement of organs between the PET and MRI studies. Pelvic organs may show little respiratory movement, but urinary volume and location of gas in the intestine, colon, and rectum may affect the location of surrounding organs. Another limitation of the present study is that pelvic MR images but not whole-body MR images were used for PET/MRI fusion images. Therefore, only the primary lesions and surrounding organs in the pelvis were evaluated. For a comparative study of diagnostic ability for metastasis, whole-body MRI is needed for the fusion images. Inline PET/MRI is expected to minimize these drawbacks of the PET/MRI fusion strategy, and several groups are developing a PET/MRI technique for experimental studies and clinical use.[20,21] Another limitation is that only two readers visually evaluated the images by subjective scoring. The evaluation depends on the reader's ability and individual impression. In addition, our patients had mostly cervical cancer, with the other cancers being represented by only three cases each. Therefore, our conclusion may be limited to cervical cancer and not be applied to general gynecological malignancies.

Conclusion

The results of our study demonstrate that MRI T2WI was superior to CT and MRI T1WI in localizing FDG accumulation and in convincingly diagnosing uterine and ovarian cancer.

Acknowledgments. This study was partly supported by the Molecular Imaging Program from the Ministry of Education, Culture, Sports, Science, and Technology (MEXT), Japan and by the Research Promotion Program on Health from the National Institute of Biomedical Innovation, Japan.

References

1. Blodgett TM, Meltzer CC, Townsend DW. PET/CT: form and function. Radiology 2007;242:360–85.
2. Kluetz PG, Meltzer CC, Villemagne VL, Kinahan PE, Chander S, Martinelli MA, et al. Combined PET/CT imaging in oncology: impact on patient management. Clin Positron Imaging 2000;3:223–30.
3. Pui MH, Wang QY, Xu B, Fan GP. MRI of gynecological neoplasm. Clin Imaging 2004;28:143–52.
4. Nicolet V, Carignan L, Bourdon F, Prosmanne O. MR imaging of cervical carcinoma: a practical staging approach. Radiographics 2000;20:1539–49.
5. Imaoka I, Wada A, Kaji Y, Hayashi T, Hayashi M, Matsuo M, et al. Developing an MR imaging strategy for diagnosis of ovarian masses. Radiographics 2006;26:1431–48.
6. Rosset A, Spadola L, Ratib O. Osiri X. An open-source software for navigating in multidimensional DICOM images. J Digit Imaging 2004;17:205–16.
7. Kim SH, Choi BI, Han JK, Kim HD, Lee HP, Kang SB, et al. Preoperative staging of uterine cervical carcinoma: comparison of CT and MRI in 99 patients. J Comput Assist Tomogr 1993;17:633–40.
8. Varpula MJ, Klemi PJ. Staging of uterine endometrial carcinoma with ultra-low field (0.02 T) MRI: a comparative study with CT. J Comput Assist Tomogr 1993;17:641–7.
9. Hricak H, Gatsonis C, Coakley FV, Snyder B, Reinhold C, Schwartz LH, et al. Early invasive cervical cancer: CT and MR imaging in preoperative evaluation: ACRIN/GOG comparative study of diagnostic performance and interobserver variability. Radiology 2007;245:491–8.
10. Rieber A, Nussle K, Stohr I, Grab D, Fenchel S, Kreienberg R, et al. Preoperative diagnosis of ovarian tumors with MR imaging: comparison with transvaginal sonography, positron emission tomography, and histologic findings. AJR Am J Roentgenol 2001;177:123–9.
11. Basu S, Li G, Alavi A. PET and PET-CT imaging of gynecological malignancies: present role and future promise. Expert Rev Anticancer Ther 2009;9:75–96.
12. Kim SK, Choi HJ, Park SY, Lee HY, Seo SS, Yoo CW, et al. Additional value of MR/PET fusion compared with PET/CT in the detection of lymph node metastases in cervical cancer patients. Eur J Cancer 2009;45:2103–9.
13. Park JY, Kim EN, Kim DY, Suh DS, Kim JH, Kim YM, et al. Comparison of the validity of magnetic resonance imaging and positron emission tomography/computed tomography in the preoperative evaluation of patients with uterine corpus cancer. Gynecol Oncol 2008;108:486–92.
14. Zasadny KR, Wahl RL. Standardized uptake values of normal tissues at PET with 2-[fluorine-18]-fluoro-2-deoxy-D-glucose: variations with body weight and a method for correction. Radiology 1993;189:847–50.
15. Liu Y. Benign ovarian and endometrial uptake on FDG PET-CT: patterns and pitfalls. Ann Nucl Med 2009;23:107–12.
16. Yen TC, See LC, Lai CH, Tsai CS, Chao A, Hsueh S, et al. Standardized uptake value in para-aortic lymph nodes is a significant prognostic factor in patients with primary advanced squamous cervical cancer. Eur J Nucl Med Mol Imaging 2008;35:493–501.
17. Lai CH, Huang KG, See LC, Yen TC, Tsai CS, Chang TC, et al. Restaging of recurrent cervical carcinoma with dual-phase [^{18}F]fluoro-2-deoxy-D-glucose positron emission tomography. Cancer 2004;100:544–52.
18. Mawlawi O, Erasmus JJ, Munden RF, Pan T, Knight AE, Macapinlac HA, et al. Quantifying the effect of IV contrast media on integrated PET/CT: clinical evaluation. AJR Am J Roentgenol 2006;186:308–19.
19. Kitajima K, Murakami K, Yamasaki E, Kaji Y, Fukasawa I, Inaba N, et al. Diagnostic accuracy of integrated FDG-PET/contrast-enhanced CT in staging ovarian cancer: comparison with enhanced CT. Eur J Nucl Med Mol Imaging 2008;35:1912–20.
20. Judenhofer MS, Catana C, Swann BK, Siegel SB, Jung WI, Nutt RE, et al. PET/MR images acquired with a compact MR-compatible PET detector in a 7-T magnet. Radiology 2007;244:807–14.
21. Imaizumi M, Yamamoto S, Kawakami M, Aoki M. Simultaneous imaging of magnetic resonance imaging and positron emission tomography by means of MRI-compatible optic fiber based PET: a validation study in ex vivo rat brain. Jpn J Radiol 2009;27:252–6.

Cancer Science
The official journal of the Japanese Cancer Association

High frequencies of less differentiated and more proliferative WT1-specific CD8$^+$ T cells in bone marrow in tumor-bearing patients: An important role of bone marrow as a secondary lymphoid organ

Ayako Murao,[1] Yoshihiro Oka,[1] Akihiro Tsuboi,[2] Olga A. Elisseeva,[3] Yukie Tanaka-Harada,[1] Fumihiro Fujiki,[3] Hiroko Nakajima,[3] Sumiyuki Nishida,[2] Naoki Hosen,[4] Toshiaki Shirakata,[5] Nobuyuki Hashimoto,[6] Akira Myoui,[7] Takafumi Ueda,[8] Yoshito Takeda,[1] Tadashi Osaki,[9] Takayuki Enomoto,[10] Hideki Yoshikawa,[6] Tadashi Kimura,[10] Yusuke Oji,[5] Ichiro Kawase[1] and Haruo Sugiyama[3,11]

Departments of [1]Respiratory Medicine, Allergy and Rheumatic Diseases, [2]Cancer Immunotherapy, [3]Functional Diagnostic Science, [4]Cancer Stem Cell Biology, [5]Biomedical Informatics, [6]Orthopaedics, Osaka University Graduate School of Medicine, Osaka; [7]Medical Center for Translational Research, Osaka University Hospital, Osaka; [8]National Hospital Organization Osaka National Hospital, Osaka; [9]Kinki Central Hospital of Mutual Aid Association of Public School Teachers, Itami; [10]Department of Obstetrics and Gynecology, Osaka University Graduate School of Medicine, Osaka, Japan

(Received August 29, 2009/Revised December 2, 2009/Accepted December 4, 2009/Online publication February 5, 2010)

In tumor-bearing patients, tumor-associated antigen (TAA)-specific CTLs are spontaneously induced as a result of immune response to TAAs and play an important role in anti-tumor immunity. Wilms' tumor gene 1 (*WT1*) is overexpressed in various types of tumor and WT1 protein is a promising pan-TAA because of its high immunogenicity. In this study, to clarify the immune response to the WT1 antigen, WT1-specific CD8$^+$ T cells that were spontaneously induced in patients with solid tumor were comparatively analyzed in both bone marrow (BM) and peripheral blood (PB). WT1-specific CD8$^+$ T cells more frequently existed in BM than in PB, whereas frequencies of naïve (CCR7$^+$ CD45RA$^+$), central memory (CCR7$^+$ CD45RA–), effector-memory (CCR7– CD45RA$^-$), and effector (CCR7– CD45RA$^+$) subsets were not significantly different between BM and PB. However, analysis of these subsets for the expression of CD57 and CD28, which were associated with differentiation, revealed that effector-memory and effector subsets of the WT1-specific CD8$^+$ T cells in BM had less differentiated phenotypes and more proliferative potential than those in PB. Furthermore, CD107a/b functional assay for WT1 peptide-specific cytotoxic potential and carboxyfluorescein diacetate succinimidyl ester dilution assay for WT1 peptide-specific proliferation also showed that WT1-specific CD8$^+$ T cells in BM were less cytotoxic and more proliferative in response to WT1 peptide than those in PB. These results implied that BM played an important role as a secondary lymphoid organ in tumor-bearing patients. Preferential residence of WT1-specific CD8$^+$ T cells in BM could be, at least in part, explained by higher expression of chemokine receptor CCR5, whose ligand was expressed on BM fibroblasts on the WT1-specific CD8$^+$ T cells in BM, compared to those in PB. These results should provide us with an insight into WT1-specific immune response in tumor-bearing patients and give us an idea of enhancement of clinical response in WT1 protein-targeted immunotherapy. (*Cancer Sci* 2010; 101: 848–854)

There is accumulating evidence that the immune system has the ability to recognize tumor-associated antigens (TAAs) and to eradicate the TAA-expressing malignant cells, also called 'tumor immunosurveillance'.[1,2] In tumor immunosurveillance, it is generally thought that CD8$^+$ CTLs are the main effector cells because they can effectively expand and kill malignant cells. Therefore, the most common approaches to combat tumors have centered on the induction of TAA-specific CTLs. Recent studies showed that CTLs with memory phenotypes also had potent anti-tumor activity.[3] Thus, not only the induction of effector CTLs but also maintenance of memory CTLs are required for ideal anti-tumor immune response in tumor-bearing patients. Regarding the maintenance of CTLs, infectious models using pathogens were well established. Interestingly, in chronic infection, in which antigens constitutively existed, it was reported that CTLs were continually activated by the antigens, finally resulting in exhaustion of the CTLs.[4] However, in tumor-bearing patients, TAAs constitutively exist for a long time, like the chronic infection. In contrast to patients with chronic infection, it appears that spontaneously induced TAA-specific CTLs in tumor-bearing patients are not exhausted but rather can be activated and expanded when the patients are treated with TAA peptide vaccines, because a considerable number of investigations showed the generation of TAA-specific CTLs from peripheral blood (PB) of tumor-bearing patients and an increase in CTL frequencies after treatment with TAA-specific vaccines.[5–8] This discrepancy in responsibility of CTLs between chronic infection and tumor bearing indicates the existence of a unique mechanism of maintenance of functional TAA-specific CTLs in tumor-bearing patients. Thus, to elucidate the unique mechanism, comprehensive analysis of the spontaneously induced TAA-specific CTLs is important.

Bone marrow (BM) has recently been shown to be an important site for T cell priming and reactivation, generation of T cell memory and recruitment of large amounts of circulating memory T cells and antigen-loaded dendritic cells (DCs).[9–13] Memory CD8$^+$ T cells in BM are more activated than those in the lymphoid periphery, and it was proposed that memory CD8$^+$ T cells in BM might receive stimulation from BM-resident cells through cell–cell contact or cytokines such as interleukin (IL)-7 or -15, resulting in their long-term maintenance in BM.[12,14–18] These findings indicated that BM was a crucial organ for migration of mature T cells and greatly contributed to long-term T cell memory. However, these findings mainly resulted from the analysis of immune responses to foreign pathogens such as virus, and the role of BM in immune response to self-antigens such as TAAs has not been investigated in detail.

Wilms' tumor gene (*WT1*), which has an oncogenic function, is highly expressed in various kinds of hematological malignancies and solid tumors.[19–23] Previous studies indicated that

[11]To whom correspondence should be addressed.
E-mail: sugiyama@sahs.med.osaka-u.ac.jp

doi: 10.1111/j.1349-7006.2009.01468.x

Table 1. Profile of patients who participated in this study

Pt. No.	Age, years/sex	Disease	Clinical stage	Prior treatments
1	56/F	Ovarian cancer (Serous papillary adenocarcinoma)	IIIc	Chemo
2	72/F	Ovarian cancer (Carcinosarcoma)	II	Chemo
3	16/F	Osteosarcoma	II	Chemo/TAE
4	51/M	Soft-tissue sarcoma(Clear cell sarcoma)	IV	Chemo/TAE
5	63/M	Lung cancer(Squamous cell carcinoma)	IIIb	Chemo/RT
6	74/M	Lung cancer(Adenocarcinoma)	IV	Chemo/RT
7	74/M	Lung cancer (Squamous cell carcinoma)	IV	Ope/RT

Chemo, chemotherapy; F, female; M, male; Ope, operation; Pt., patient; RT, radiation therapy; TAE, transcatheter arterial embolization.

stimulation of PBMCs with MHC class I-restricted WT1 protein-derived peptides induced WT1-specific $CD8^+$ T cells in an MHC class I-restricted manner, and the induced WT1-specific $CD8^+$ T cells specifically killed WT1-expressing tumor cells without affecting normal cells that physiologically expressed WT1, indicating that WT1 could be a promising target antigen for cancer immunotherapy.[22–27] WT1-specific $CD8^+$ T cells and WT1 IgM and IgG antibodies were spontaneously induced in patients with WT1-expressing tumors.[28] Clinical trials of WT1 peptide vaccination are now being carried out for patients with various types of malignancies, and WT1-specific $CD8^+$ T cell responses and the resultant clinical responses have been reported.[5,21,29–34] However, detailed analysis of spontaneously induced WT1-specific $CD8^+$ T cells in tumor-bearing patients has not yet been done. Furthermore, the majority of the findings resulted from the analysis of PB, and there is little data about WT1-specific $CD8^+$ T cells in BM, an important site for immune response to TAAs. Therefore, detailed comparative analysis of WT1-specific $CD8^+$ T cells in both PB and BM is interesting and necessary to understand further the WT1-directed immune responses, which should lead to enhancement of the clinical response of WT1 protein-targeted immunotherapy.

In the present study, we comparatively analyzed WT1-specific $CD8^+$ T cells in BM and PB in solid tumor-bearing patients using multicolor flowcytometry for cell surface differentiation markers, CD107a/b functional assay for WT1 peptide-specific cytotoxic potential, and carboxyfluorescein diacetate succinimidyl ester (CFSE) dilution assay for WT1 peptide-specific proliferation, and describe that WT1-specific $CD8^+$ T cells in BM are less differentiated and more proliferative than those in PB, implying an important role of BM as a secondary lymphoid organ.

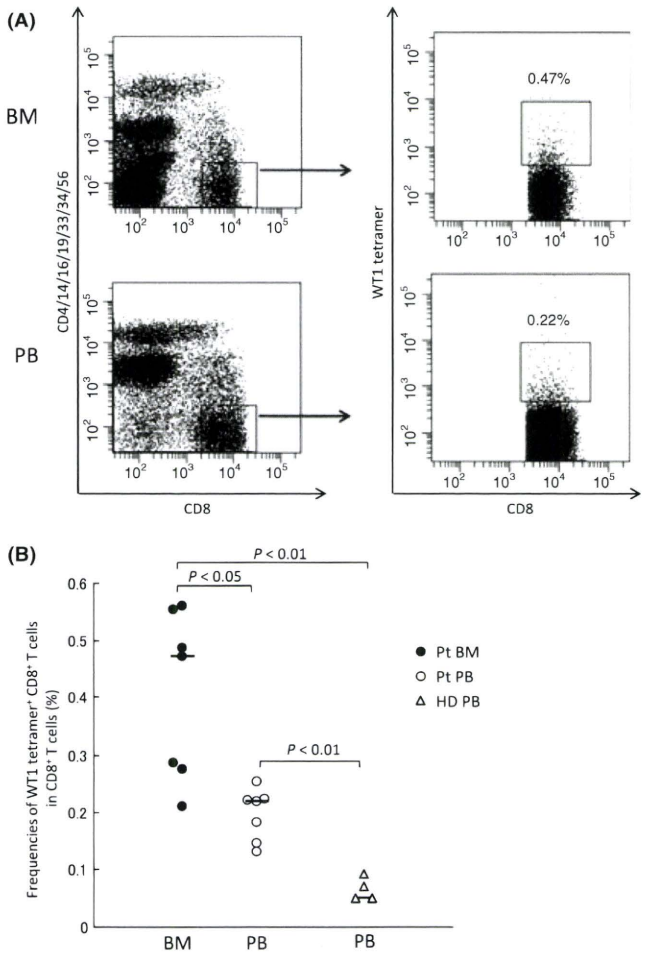

Fig. 1. Frequencies of WT1 tetramer$^+$ $CD8^+$ T cells in bone marrow (BM) and peripheral blood (PB) in patients with solid tumors. (A) Representative flow cytometric analysis of WT1 tetramer$^+$ $CD8^+$ T cells. Mononuclear cells from BM and PB were gated on $CD8^+$, $CD4^-$, $CD14^-$, $CD16^-$, $CD19^-$, $CD33^-$, $CD34^-$, and $CD56^-$ cells, and WT1 tetramer$^+$ $CD8^+$ T cells were defined as WT1-specific $CD8^+$ T cells. (B) Frequencies of WT1 tetramer$^+$ $CD8^+$ T cells in $CD8^+$ T cells in BM (closed circles) and PB (open circles) from patients (Pt), and PB from healthy donors (HD; open triangles). The horizontal bars indicate median values of the frequencies.

Materials and Methods

Patients and healthy donors. Three patients with lung cancer, two patients with ovarian cancer, one patient with osteosarcoma, and one patient with soft-tissue sarcoma were analyzed (Table 1). *WT1* expression in tumor cells was determined by immunohistochemistry. No bone marrow metastasis was detected in any patient. After written informed consent was given, PB and BM samples were obtained from seven HLA-A*2402$^+$ patients. PB samples were also obtained from four HLA-A*2402$^+$ healthy donors. PBMCs and BM mononuclear cells (BMMCs) were isolated by density gradient centrifugation using Ficoll–Hypaque and cryopreserved until analysis.

Flow cytometric analysis. PBMCs and BMMCs were incubated with phycoerythrin (PE)-conjugated HLA-A*2402/$WT1_{235–243}$ tetramer (MBL, Tokyo, Japan) in FACS buffer composed of PBS and 5% FBS at 37°C for 30 min. Subsequently, these cells were stained with a mixture of mAbs: (a) anti-CD8-APC-Cy7 (BD Biosciences, San Diego, CA, USA), anti-CD45RA-ECD (Beckman Coulter, Marseille, France), anti-CCR7-PE-Cy7 (BD Biosciences), FITC-labeled-anti-CD4 (Biolegend, San Diego, CA, USA), -CD14 (BD Biosciences), -CD16 (eBioscience, San Diego, CA, USA), -CD19, -CD33, -CD34 (all BD Biosciences), and -CD56 (eBioscience); or (b) anti-CD8-APC-Cy7, anti-CD45RA-ECD, anti-CCR7-PE-Cy7, anti-CD57-APC (Biolegend), and anti-CD28-FITC (eBioscience), at

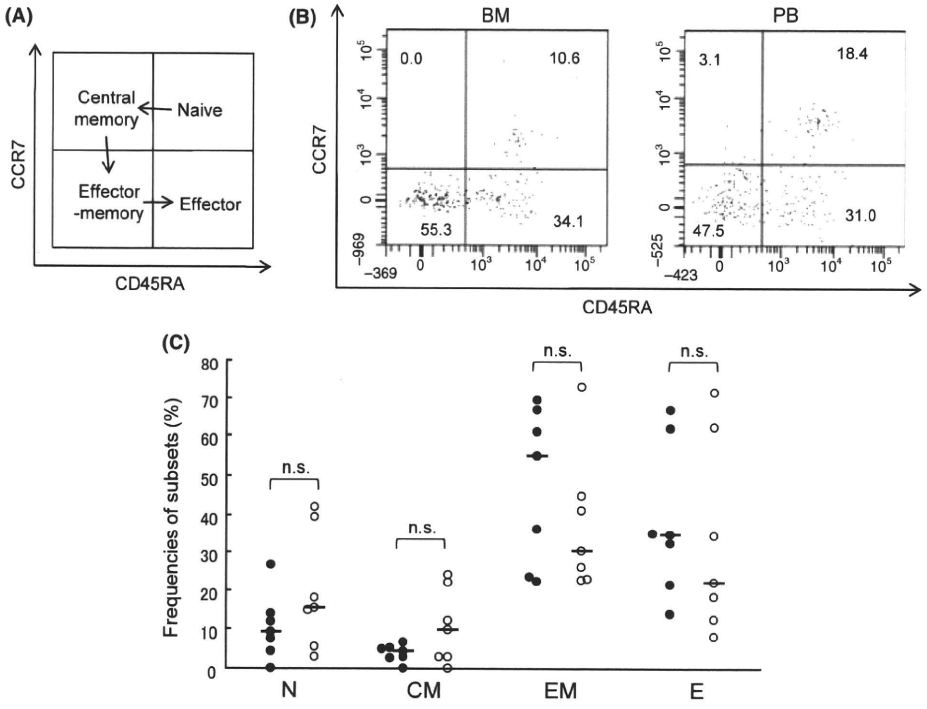

Fig. 2. Subset composition of WT1 tetramer$^+$ CD8$^+$ T cells in bone marrow (BM) and peripheral blood (PB). (A) WT1 tetramer$^+$ CD8$^+$ T cells are divided into four subsets according to the expression of CCR7 and CD45RA and differentiate as follows: naïve (N), CCR7$^+$ CD45RA$^+$ → central memory (CM), CCR7$^+$ CD45RA$^-$ → effector- memory (EM), CCR7$^-$ CD45RA$^-$ → effector (E), CCR7$^-$ CD45RA$^+$. (B) Representative subset analysis of WT1 tetramer$^+$ CD8$^+$ T cells in BM and PB. Frequencies of N, CM, EM, and E subsets are shown. (C), Frequencies of each subset of WT1 tetramer$^+$ CD8$^+$ T cells in BM (closed circles) and PB (open circles) are shown. The horizontal bars indicate median values of the frequencies.

4°C for 20 min, washed three times, and resuspended in FACS buffer. In staining with (a), CD8$^+$ and CD4$^-$, CD14$^-$, CD16$^-$ CD19$^-$, CD33$^-$, CD34$^-$, and CD56$^-$ cells were defined as CD8$^+$ T cells. CD8^{low+} cells, in which natural killer (NK) cells were contaminated, were gated out from the gating for CD8$^+$ T cells, because cells tended to give rise to non-specific binding to WT1 tetramer. Data acquisition was carried out on a FACSAria instrument (BD Biosciences), and the data were analyzed using FACSDiva software (BD Biosciences).

CD107a/b assay. PBMCs and BMMCs were stimulated *in vitro* with 10 μg/mL natural 9-mer $WT1_{235}$ peptide or mERK (QYIHSANVL) peptide (irrelevant peptide) in the presence of BD GolgiStop (BD Biosciences) and FITC-conjugated mAbs for CD107a and CD107b (BD Biosciences) for 3 h. The cells were then harvested, washed, stained with mAbs for anti-CD8-APC-Cy7, anti-CD45RA-ECD, and anti-CCR7-PE-Cy7, and gated on lymphocytes. Frequencies of CD107a/b$^+$ cells induced specifically by WT1 peptide stimulation were calculated by subtracting the frequencies of CD107a/b$^+$ cells induced by irrelevant mERK peptide stimulation from those of CD107a/b$^+$ cells induced by WT1 peptide stimulation.

Proliferation assay. Proliferative potential of WT1 peptide-specific CTLs was examined according to previous reports.[35] Briefly, PBMC and BMMC were labeled with 2.5 μM CFSE (Molecular Probes, Eugene, OR, USA), and 2×10^5 cells were plated in 96-well round plates in 100 μL X-VIVO 15 with 5% AB serum. The cells were stimulated with natural 9-mer $WT1_{235-243}$ peptide at a concentration of 10 μg/mL. After 2 days of culture, 100 μL X-VIVO 15 medium with 5% AB serum containing IL-2 (100 IU/mL) was added. After 10 days of peptide stimulation, the cells were re-stimulated for 6 h with or without the WT1 peptide (10 μg/mL), with the addition of 10 μg/mL Brefeldin A (SIGMA) for the last 5 h to block cytokine secretion. After 6 h of WT1 peptide stimulation, cells were washed, stained with anti-CD8-APC-Cy-7 and anti-CD3-PerCP, fixed, permeabilized, and stained with anti-interferon (IFN)-γ-APC. CD3$^+$ CD8$^+$ IFN-γ$^+$ cells were analyzed for CFSE dilution.

Statistical analysis. Differences between test groups were analyzed using the Mann–Whitney *U*-test.

Results

Bone marrow contains WT1-specific CD8$^+$ T cells at higher frequencies than PB in patients with solid tumor. Frequencies of WT1 tetramer$^+$ CD8$^+$ T cells in total CD8$^+$ T cells were measured in BM and PB by staining the mononuclear cells with HLA-A*2402/WT1 tetramer. BMMCs and PBMCs from seven HLA-A*2402$^+$ patients with solid tumor were examined (Table 1 and Fig. 1). The frequencies of WT1 tetramer$^+$ CD8$^+$ T cells in CD8$^+$ T cells were significantly higher in BM than in PB (median, 0.47% *vs* 0.22%; $P < 0.05$) (Fig. 1B). For reference, PB from four HLA-A*2402$^+$ healthy donors were similarly examined. Frequencies of WT1 tetramer$^+$ CD8$^+$ T cells in PB were significantly lower than those in BM and PB of seven patients (median, 0.05% [PB in healthy donors] *vs* 0.47% [BM in patients], 0.22% [PB in patients]; $P < 0.01$) (Fig. 1B), which was consistent with previous reports.[5]

Effector-memory and effector subsets of WT1-specific CD8$^+$ T cells in BM had less differentiated and more proliferative phenotypes than those in PB. To elucidate whether the WT1-specific CD8$^+$ T cells in BM phenotypically differed from those in PB, WT1-specific CD8$^+$ T cells are phenotypically classified into four distinct differentiation stages based on surface expression of CCR7 and CD45RA: naïve (N), CCR7$^+$ CD45RA$^+$; central memory (CM), CCR7$^+$ CD45RA$^-$; effector-memory (EM),

doi: 10.1111/j.1349-7006.2009.01468.x

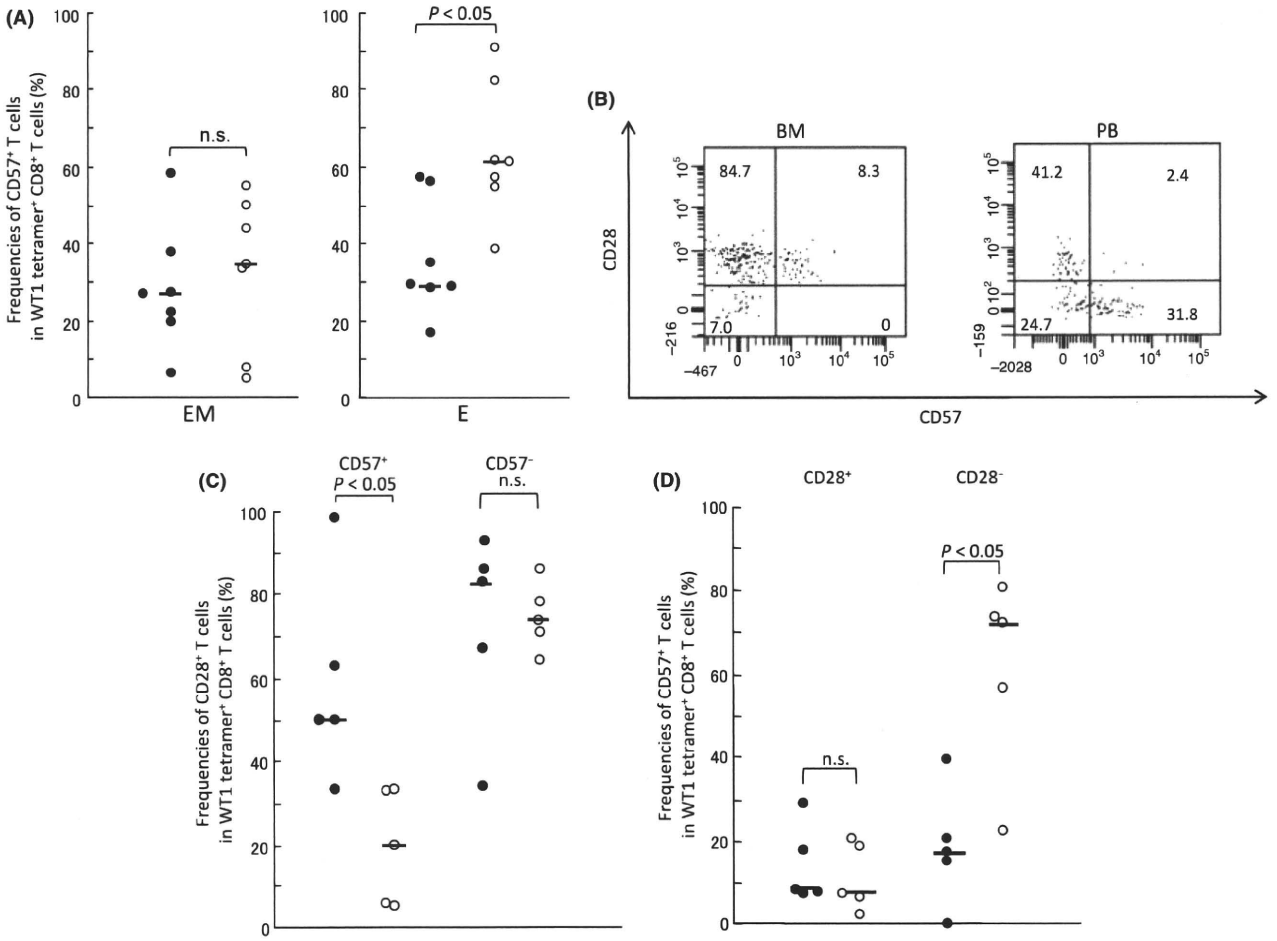

Fig. 3. Effector-memory (EM) and effector (E) subsets of WT1 tetramer$^+$ CD8$^+$ T cells in bone marrow (BM) had less differentiated and more proliferative phenotypes than those in peripheral blood (PB). (A) Frequencies of CD57$^+$ cells in EM and E subsets of WT1 tetramer$^+$ CD8$^+$ T cells in BM (closed circles) and PB (open circles). (B) Representative dot-plots of FACS analysis of CD28 and CD57 expression in the EM subset. Numbers represent frequencies (%) of cells in each fraction. (C) Frequencies of CD28$^+$ T cells in the CD57$^+$ or CD57$^-$ EM subset in WT1 tetramer$^+$ CD8$^+$ T cells in BM (closed circles) and PB (open circles). (D) Frequencies of CD57$^+$ T cells in the CD28$^+$ or CD28$^-$ EM subset in WT1 tetramer$^+$ CD8$^+$ T cells in BM (closed circles) and PB (open circles). Two patients were not evaluated because of the small number of cells. Horizontal bars indicate median values of the frequencies. n.s., not significant.

CCR7$^-$ CD45RA$^-$; and effector (E), CCR7$^-$ CD45RA$^+$.[36,37] It is well known that CD8$^+$ T cells differentiate as follows: N $\rightarrow$ CM $\rightarrow$ EM $\rightarrow$ E (Fig. 2A). As shown in Figure 2B, the majority of the WT1 tetramer$^+$ CD8$^+$ T cells belonged to EM and E subsets, and there was no significant difference in the frequencies of N, CM, EM, and E subsets of WT1 tetramer$^+$ CD8$^+$ T cells between BM and PB (Fig. 2C).

Subsets EM and E of WT1 tetramer$^+$ CD8$^+$ T cells, which accounted for the majority of the T cells, were further examined for the expression of CD57. Low CD57 expression means that cells are less differentiated and have sufficient proliferative potential. As shown in Figure 3A, frequencies of CD57$^+$ cells in E subset of WT1 tetramer$^+$ CD8$^+$ T cells were lower in BM than in PB (median, 28.5% *vs* 61.0%; $P < 0.05$). However, frequencies of CD57$^+$ cells in EM subset of WT1 tetramer$^+$ CD8$^+$ T cells were not significantly different between BM and PB. These results indicated that E subset of WT1 tetramer$^+$ CD8$^+$ T cells in BM had less differentiated and more proliferative phenotypes than that in PB.

Next, EM subset of WT1 tetramer$^+$ CD8$^+$ T cells, in which no significant difference in CD57 expression was found between BM and PB, was further examined for the expression of CD28, whose high expression means less differentiated state and sufficient proliferative potential (Fig. 3).[38,39] In CD57$^+$ cells in EM subset, CD28$^+$ cells (less differentiated) were more in BM than in PB (median, 50.0% *vs* 20.0%; $P < 0.05$), whereas in CD28$^-$ cells in EM subset, CD57$^+$ cells (more differentiated) were less in BM than in PB (median, 16.6% *vs* 71.4%; $P < 0.05$) (Fig. 3C,D). These results showed that WT1 tetramer$^+$ CD8$^+$ T cells in EM subset also had less differentiated phenotype in BM than in PB. Taken together, these results indicated that both EM and E subsets of WT1 tetramer$^+$ CD8$^+$ T cells in BM had less differentiated and more proliferative phenotypes than those of WT1 tetramer$^+$ CD8$^+$ T cells in PB.

WT1-specific CD8$^+$ T cells in BM have higher proliferative potential than those in PB. As we demonstrated that EM and E subsets of WT1-specific CD8$^+$ T cells in BM had less differentiated and more proliferative phenotypes than those in PB, proliferative activity of WT1-specific CD8$^+$ T cells was examined. CFSE-labeled BMMCs and PBMCs were stimulated with WT1 peptide. After 10 days of the peptide stimulation, expanded BMMCs and PBMCs were restimulated with WT1 peptide for

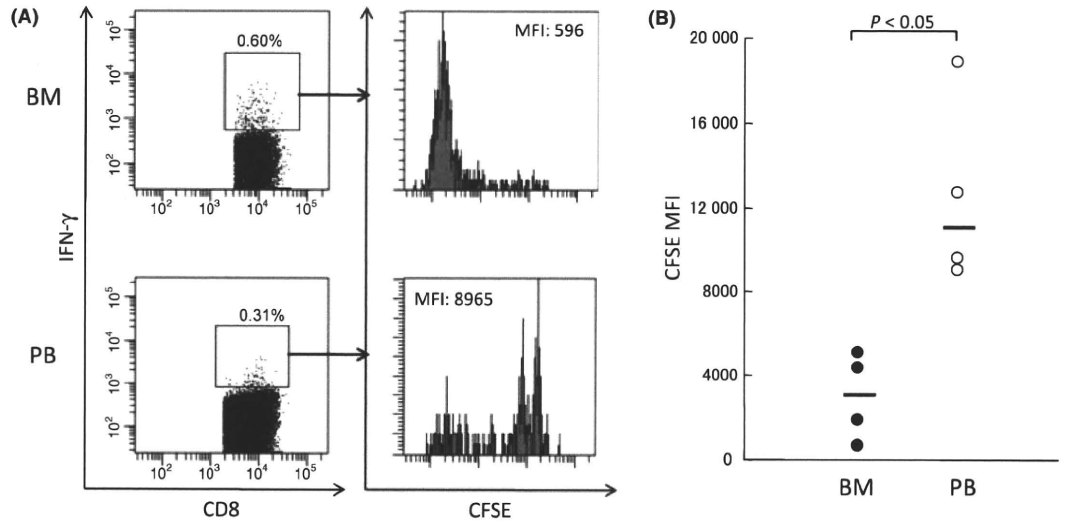

Fig. 4. Proliferative potential of WT1-reactive CD8$^+$ T cells. Carboxyfluorescein diacetate succinimidyl ester (CFSE)-labeled bone marrow (BM) and peripheral blood (PB) mononuclear cells were stimulated with WT1 peptides, and CFSE dilution was analyzed by FACS. (A) Representative flow cytometric analysis of CFSE dilution in interferon (IFN)-γ^+ CD8$^+$ CD3$^+$ T cells. (B) CFSE mean fluorescence intensity (MFI) of IFN-γ^+ CD8$^+$ CD3$^+$ T cells in BM (closed circles) and PB (open circles). Horizontal bars indicate median values of MFI.

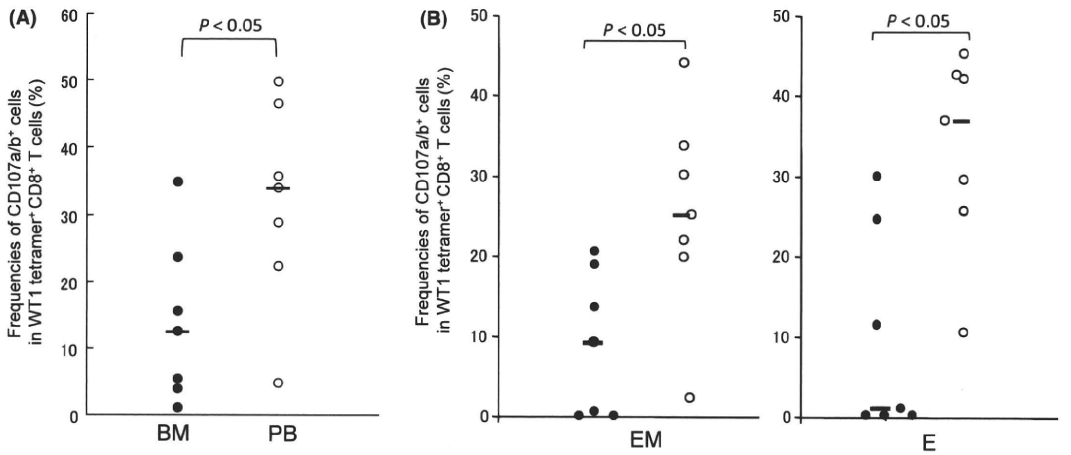

Fig. 5. Cytotoxic potential of WT1 tetramer$^+$ CD8$^+$ T cells. Mononuclear cells from bone marrow (BM) and peripheral blood (PB) were stimulated with WT1 peptide, then CD107a/b cell surface expression was examined. (A) Frequencies of CD107a/b$^+$ cells in WT1 tetramer$^+$ CD8$^+$ T cells in BM (closed circles) and PB (open circles). (B) Frequencies of CD107a/b$^+$ cells in effector-memory (EM) and effector (E) subsets in WT1 tetramer$^+$ CD8$^+$ T cells in BM (closed circles) and PB (open circles). Horizontal bars indicate median values of the frequencies.

6 h and analyzed for CFSE dilution in WT1 peptide-responding IFN-γ^+ CD3$^+$ CD8$^+$ cells (Fig. 4). A substantial number of IFN-γ^+ cells were detected after the stimulation with WT1 peptide (Fig. 4A), but only a few IFN-γ^+ cells were detected without the stimulation (negative control; data not shown). CFSE dilution profile of the IFN-γ^+ cells and its mean fluorescence intensity (MFI, 3008.5 [PB] *vs* 11 051 [BM]; $P < 0.05$) showed that IFN-γ^+ CD3$^+$ CD8$^+$ cells in BM were more proliferative than those in PB (Fig. 4B). These results indicated that WT1-specific CD8$^+$ T cells in BM had higher proliferative potential than those in PB.

WT1-specific CD8$^+$ T cells in BM have lower cytotoxic potential than those in PB. Cytotoxic potential of WT1 tetramer$^+$ CD8$^+$ T cells was analyzed by CD107a/b assay, because the assay was shown to strongly correlate with killing activity of CTLs.[40] BMMCs and PBMCs were stimulated with WT1 peptide or mERK irrelevant peptide, then frequencies of CD107a/b-expressing cells were examined. As shown in Figure 5A, the frequencies of CD107a/b-expressing cells in WT1 tetramer$^+$ CD8$^+$ T cells were lower in BM than in PB (median, 12.4% *vs* 33.7%; $P < 0.05$). Furthermore, CD107a/b expression on EM and E subsets of WT1 tetramer$^+$ CD8$^+$ T cells was investigated in BM and PB. As shown in Figure 5B, frequencies of CD107a/b-expressing cells in EM and E subsets of WT1 tetramer$^+$ CD8$^+$ T cells were significantly lower in BM than in PB (EM, 9.1% *vs* 25.0%, $P < 0.05$; E, 0.8% *vs* 36.7%, $P < 0.05$). These results strongly indicated that WT1-specific cytotoxic potential of WT1-specific CD8$^+$ T cells in BM was lower than that of WT1-specific CD8$^+$ T cells in PB.

doi: 10.1111/j.1349-7006.2009.01468.x

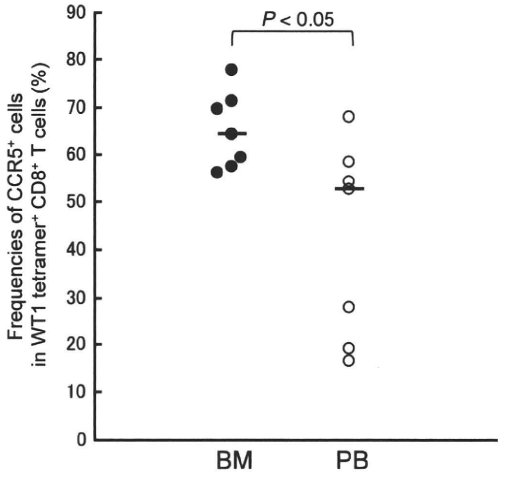

Fig. 6. Expression of chemokine receptor CCR5 on WT1 tetramer$^+$ CD8$^+$ T cells. Frequencies of CCR5$^+$ cells in WT1 tetramer$^+$ CD8$^+$ T cells in bone marrow (BM; closed circles) and peripheral blood (PB; open circles). Horizontal bars indicate median values of the frequencies.

Expression of chemokine receptor CCR5 on WT1-specific CD8$^+$ T cells higher in BM than in PB. Expression levels of chemokine receptors CCR5 and CXCR4 on WT1 tetramer$^+$ CD8$^+$ T cells were examined in BM and PB. As shown in Figure 6, frequencies of CCR5$^+$ cells in WT1 tetramer$^+$ CD8$^+$ T cells were significantly higher in BM than in PB (median, 64.3% *vs* 52.5%; $P < 0.05$). Frequencies of CXCR4$^+$ cells in WT1 tetramer$^+$ CD8$^+$ T cells tended to be higher in BM than in PB, although they were not statistically significant (median, 49.3% *vs* 35.7%, not significant) (data not shown). Ligands CCL5 and SDF-1 for chemokine receptors CCR5 and CXCR4, respectively, are highly expressed in the BM microenvironment and play an important role in interaction between the cells with these chemokine receptors and the BM microenvironment. Therefore, these results, at least in part, gave us an explanation for the preferential residence of WT1-specific CD8$^+$ T cells in BM compared to PB.

Discussion

The present study showed for the first time the characterization of WT1-specific CD8$^+$ T cells that were spontaneously induced as a result of stimulating the immune system by highly WT1-expressing tumor cells in patients with solid tumor. In comparison with WT1-specific CD8$^+$ T cells in PB, those in BM were higher in frequency, less differentiated, and more proliferative, and had less cytotoxic potential. The preferential residence of WT1-specific CD8$^+$ T cells in BM could be explained, at least in part, by the higher expression of chemokine receptors CCR5 and CXCR4 on WT 1-specific CD8$^+$ T cells in BM compared to WT1-specific CD8$^+$ T cells in PB.

Our results allowed us to consider that BM provided an important site for priming and reactivation of CD8$^+$ T cells with TAAs, that is, BM functioned as a secondary lymphoid organ. It has been reported that differentiated DCs constitutively traffic from peripheral tissues to blood and the circulating DCs home with a rather high tropism to BM, where the DCs activate naïve and resident T cells.[10–13,41] Therefore, it appeared that DCs that captured WT1 antigen, which was produced from WT1-expressing tumor cells, in peripheral sites homed to BM, presented the WT1 antigen to circulating naïve CD8$^+$ T cells and resident CD8$^+$ T cells and activated them. It then seems that the activated WT1-specific CD8$^+$ T cells differentiated into the CD8$^+$ T cells with more matured phenotypes, which finally migrated from BM to tumor sites through PB and exerted cytotoxic activity there. Others analyzed MUC-1- or Her2/neu-specific CD8$^+$ T cells that were spontaneously induced in tumor-bearing patients by using the corresponding tetramers and reported no difference in the frequencies of the CD8$^+$ T cells between BM and PB.[42,43] However, as further detailed analysis of the CD8$^+$ T cells was not done in these studies, the cause of the discrepancy between our results and theirs cannot be discussed in detail.

Concerning another aspect of BM function, a number of reports showed that BM was a pooling site of memory T cells.[12,14,16,18,41,44–49] Adoptive T cell transfer studies showed that memory T cells migrated to BM and preferentially proliferated there through the signals by cytokines such as IL-7 and IL-15.[14,16] Thus, BM plays an important role in the maintenance of memory T cells. Our present study also showed that WT1-specific effector-memory and effector CD8$^+$ T cells accumulated in BM in patients with WT1-expressing solid tumor. Furthermore, our detailed phenotype analysis showed that WT1-specific CD8$^+$ T cells in E and EM subsets in BM had unique phenotypes, such as less differentiated state, more proliferative potential, and less cytotoxic, compared to those in E and EM subsets in PB. T cells with low expression of CD57 and high expression of CD28 are considered to sustain sufficient proliferative potential and less cytotoxic potential. Conversely, high expression of CD57 and low expression of CD28 are associated with replicatively senescent T cells and clonally exhausted T cells with cytotoxic potential, respectively.[38,39,50–52] In the T cells with these characteristics, T-cell receptor management extra circles (TREC) levels were very low and telomere lengths were shortened, and hence these T cells apoptose by antigen stimulation.[39,53] Therefore, our phenotype analysis suggested that WT1-specific CD8$^+$ T cells in EM and E subsets in BM sustained more sufficient proliferative potential and less cytotoxic potential, compared to those in EM and E subsets in PB. CD107a/b assay, a functional assay to examine cytotoxicity, also revealed that WT1-specific CD8$^+$ T cells in BM had less cytotoxic potential than those in PB, consistent with the results of the phenotype analysis of CD57 and CD28 expression. In the CD107a/b assay presented here, whole BMMCs and PBMCs were used. To confirm our present results, CD107a/b assay was applied to EM and E subsets FACS-sorted from another patient. As expected, frequencies of CD107a/b-expressing cells in WT1 tetramer$^+$ CD8$^+$ T cells in purified EM and E subsets were lower in BM than in PB, confirming our results. Furthermore, proliferation assay by CFSE dilution that showed higher proliferative potential of WT1-specific CD8$^+$ T cells in BM than in PB was also compatible with the results of phenotype analysis. These results suggested that WT1-specific CD8$^+$ T cells with more proliferative and less cytotoxic potential could be maintained in the BM until they are reactivated by DCs.

WT1-specific CD8$^+$ T cells in BM expressed chemokine receptors CCR5 and CXCR4 at higher frequencies than those in PB. CCL3 and CCL5, ligands for CCR5, were expressed on BM fibroblasts, and CXCL12, a ligand for CXCR4, was produced on BM stromal cells and endothelium of BM microvessels.[54–56] Therefore, preferential homing and localization of WT1-specific CD8$^+$ T cells to BM should be ascribed to preferential interaction between chemokine receptors on the T cells and its ligands in the BM microenvironment. It appears to be reasonable to consider that downregulation of such chemokine receptors on the T cells promotes emigration of the T cells from BM to PB. These findings also allowed us to consider BM as a secondary lymphoid organ.

Acknowledgment

The excellent help of T. Umeda as a research nurse is acknowledged.

References

1 Dunn GP, Bruce AT, Ikeda H, Old LJ, Schreiber RD. Cancer immunoediting: from immunosurveillance to tumor escape. *Nat Immunol* 2002; **3**: 991–8.
2 Malmberg KJ, Ljunggren HG. Escape from immune- and nonimmune-mediated tumor surveillance. *Semin Cancer Biol* 2006; **16**: 16–31.
3 Klebanoff CA, Gattinoni L, Restifo NP. CD8+ T-cell memory in tumor immunology and immunotherapy. *Immunol Rev* 2006; **211**: 214–24.
4 Ibegbu CC, Xu YX, Harris W, Maggio D, Miller JD, Kourtis AP. Expression of killer cell lectin-like receptor G1 on antigen-specific human CD8+ T lymphocytes during active, latent, and resolved infection and its relation with CD57. *J Immunol* 2005; **174**: 6088–94.
5 Oka Y, Tsuboi A, Taguchi T *et al.* Induction of WT1 (Wilms' tumor gene)-specific cytotoxic T lymphocytes by WT1 peptide vaccine and the resultant cancer regression. *Proc Natl Acad Sci U S A* 2004; **101**: 13885–90.
6 Pittet MJ, Speiser DE, Lienard D *et al.* Expansion and functional maturation of human tumor antigen-specific CD8+ T cells after vaccination with antigenic peptide. *Clin Cancer Res* 2001; **7**: 796s–803s.
7 Walker EB, Haley D, Miller W *et al.* gp100(209-2M) peptide immunization of human lymphocyte antigen-A2+ stage I-III melanoma patients induces significant increase in antigen-specific effector and long-term memory CD8+ T cells. *Clin Cancer Res* 2004; **10**: 668–80.
8 Romero P, Valmori D, Pittet MJ *et al.* Antigenicity and immunogenicity of Melan-A/MART-1 derived peptides as targets for tumor reactive CTL in human melanoma. *Immunol Rev* 2002; **188**: 81–96.
9 Letsch A, Knoedler M, Na IK *et al.* CMV-specific central memory T cells reside in bone marrow. *Eur J Immunol* 2007; **37**: 3063–8.
10 Cavanagh LL, Bonasio R, Mazo IB *et al.* Activation of bone marrow-resident memory T cells by circulating, antigen-bearing dendritic cells. *Nat Immunol* 2005; **6**: 1029–37.
11 Feuerer M, Beckhove P, Garbi N *et al.* Bone marrow as a priming site for T-cell responses to blood-borne antigen. *Nat Med* 2003; **9**: 1151–7.
12 Di Rosa F, Pabst R. The bone marrow: a nest for migratory memory T cells. *Trends Immunol* 2005; **26**: 360–6.
13 Bonasio R, von Andrian UH. Generation, migration and function of circulating dendritic cells. *Curr Opin Immunol* 2006; **18**: 503–11.
14 Becker TC, Coley SM, Wherry EJ, Ahmed R. Bone marrow is a preferred site for homeostatic proliferation of memory CD8 T cells. *J Immunol* 2005; **174**: 1269–73.
15 Di Rosa F, Santoni A. Bone marrow CD8 T cells are in a different activation state than those in lymphoid periphery. *Eur J Immunol* 2002; **32**: 1873–80.
16 Parretta E, Cassese G, Barba P, Santoni A, Guardiola J, Di Rosa F. CD8 cell division maintaining cytotoxic memory occurs predominantly in the bone marrow. *J Immunol* 2005; **174**: 7654–64.
17 Cassese G, Parretta E, Pisapia L, Santoni A, Guardiola J, Di Rosa F. Bone marrow CD8 cells down-modulate membrane IL-7Ralpha expression and exhibit increased STAT-5 and p38 MAPK phosphorylation in the organ environment. *Blood* 2007; **110**: 1960–9.
18 Mazo IB, Honczarenko M, Leung H *et al.* Bone marrow is a major reservoir and site of recruitment for central memory CD8+ T cells. *Immunity* 2005; **22**: 259–70.
19 Oji Y, Miyoshi S, Maeda H *et al.* Overexpression of the Wilms' tumor gene WT1 in de novo lung cancers. *Int J Cancer* 2002; **100**: 297–303.
20 Oji Y, Ogawa H, Tamaki H *et al.* Expression of the Wilms' tumor gene WT1 in solid tumors and its involvement in tumor cell growth. *Jpn J Cancer Res* 1999; **90**: 194–204.
21 Oji Y, Suzuki T, Nakano Y *et al.* Overexpression of the Wilms' tumor gene W T1 in primary astrocytic tumors. *Cancer Sci* 2004; **95**: 822–7.
22 Oka Y, Tsuboi A, Kawakami M *et al.* Development of WT1 peptide cancer vaccine against hematopoietic malignancies and solid cancers. *Curr Med Chem* 2006; **13**: 2345–52.
23 Sugiyama H. Wilms' tumor gene WT1: its oncogenic function and clinical application. *Int J Hematol* 2001; **73**: 177–87.
24 Oka Y, Udaka K, Tsuboi A *et al.* Cancer immunotherapy targeting Wilms' tumor gene WT1 product. *J Immunol* 2000; **164**: 1873–80.
25 Oka Y, Elisseeva OA, Tsuboi A *et al.* Human cytotoxic T-lymphocyte responses specific for peptides of the wild-type Wilms' tumor gene (WT1) product. *Immunogenetics* 2000; **51**: 99–107.
26 Ohminami H, Yasukawa M, Fujita S. HLA class I-restricted lysis of leukemia cells by a CD8(+) cytotoxic T-lymphocyte clone specific for WT1 peptide. *Blood* 2000; **95**: 286–93.
27 Tsuboi A, Oka Y, Udaka K *et al.* Enhanced induction of human WT1-specific cytotoxic T lymphocytes with a 9-mer WT1 peptide modified at HLA-A*2402-binding residues. *Cancer Immunol Immunother* 2002; **51**: 614–20.
28 Elisseeva OA, Oka Y, Tsuboi A *et al.* Humoral immune responses against Wilms tumor gene WT1 product in patients with hematopoietic malignancies. *Blood* 2002; **99**: 3272–9.
29 Tsuboi A, Oka Y, Osaki T *et al.* WT1 peptide-based immunotherapy for patients with lung cancer: report of two cases. *Microbiol Immunol* 2004; **48**: 175–84.
30 Oka Y, Tsuboi A, Murakami M *et al.* Wilms tumor gene peptide-based immunotherapy for patients with overt leukemia from myelodysplastic syndrome (MDS) or MDS with myelofibrosis. *Int J Hematol* 2003; **78**: 56–61.
31 Oka Y, Tsuboi A, Elisseeva OA *et al.* WT1 peptide cancer vaccine for patients with hematopoietic malignancies and solid cancers. *ScientificWorldJournal* 2007; **7**: 649–65.
32 Izumoto S, Tsuboi A, Oka Y *et al.* Phase II clinical trial of Wilms tumor 1 peptide vaccination for patients with recurrent glioblastoma multiforme. *J Neurosurg* 2008; **108**: 963–71.
33 Iiyama T, Udaka K, Takeda S *et al.* WT1 (Wilms' tumor 1) peptide immunotherapy for renal cell carcinoma. *Microbiol Immunol* 2007; **51**: 519–30.
34 Rezvani K, Yong AS, Mielke S *et al.* Leukemia-associated antigen-specific T-cell responses following combined PR1 and WT1 peptide vaccination in patients with myeloid malignancies. *Blood* 2008; **111**: 236–42.
35 Bozzacco L, Trumpfheller C, Siegal FP *et al.* DEC-205 receptor on dendritic cells mediates presentation of HIV gag protein to CD8+ T cells in a spectrum of human MHC I haplotypes. *Proc Natl Acad Sci U S A* 2007; **104**: 1289–94.
36 Sallusto F, Lenig D, Forster R, Lipp M, Lanzavecchia A. Two subsets of memory T lymphocytes with distinct homing potentials and effector functions. *Nature* 1999; **401**: 708–12.
37 Sallusto F, Mackay CR, Lanzavecchia A. The role of chemokine receptors in primary, effector, and memory immune responses. *Annu Rev Immunol* 2000; **18**: 593–620.
38 Monteiro J, Batliwalla F, Ostrer H, Gregersen PK. Shortened telomeres in clonally expanded CD28-CD8+ T cells imply a replicative history that is distinct from their CD28 + CD8+ counterparts. *J Immunol* 1996; **156**: 3587–90.
39 Weng NP, Akbar AN, Goronzy J. CD28(−) T cells: their role in the age-associated decline of immune function. *Trends Immunol* 2009; **30**: 306–12.
40 Rubio V, Stuge TB, Singh N *et al.* Ex vivo identification, isolation and analysis of tumor-cytolytic T cells. *Nat Med* 2003; **9**: 1377–82.
41 Di Rosa F. T-lymphocyte interaction with stromal, bone and hematopoietic cells in the bone marrow. *Immunol Cell Biol* 2009; **87**: 20–9.
42 Feuerer M, Beckhove P, Bai L *et al.* Therapy of human tumors in NOD/SCID mice with patient-derived reactivated memory T cells from bone marrow. *Nat Med* 2001; **7**: 452–8.
43 Beckhove P, Feuerer M, Dolenc M *et al.* Specifically activated memory T cell subsets from cancer patients recognize and reject xenotransplanted autologous tumors. *J Clin Invest* 2004; **114**: 67–76.
44 Price PW, Cerny J. Characterization of CD4+ T cells in mouse bone marrow I. Increased activated/memory phenotype and altered TCR Vbeta repertoire. *Eur J Immunol* 1999; **29**: 1051–6.
45 Slifka MK, Whitmire JK, Ahmed R. Bone marrow contains virus-specific cytotoxic T lymphocytes. *Blood* 1997; **90**: 2103–8.
46 Zhang X, Dong H, Lin W *et al.* Human bone marrow: a reservoir for "enhanced effector memory" CD8+ T cells with potent recall function. *J Immunol* 2006; **177**: 6730–7.
47 Tokoyoda K, Zehentmeier S, Hegazy AN *et al.* Professional memory CD4+ T lymphocytes preferentially reside and rest in the bone marrow. *Immunity* 2009; **30**: 721–30.
48 Racanelli V, Frassanito MA, Leone P, Brunetti C, Ruggieri S, Dammacco F. Bone marrow of persistently hepatitis C virus-infected individuals accumulates memory CD8+ T cells specific for current and historical viral antigens: a study in patients with benign hematological disorders. *J Immunol* 2007; **179**: 5387–98.
49 Palendira U, Chinn R, Raza W *et al.* Selective accumulation of virus-specific CD8+ T cells with unique homing phenotype within the human bone marrow. *Blood* 2008; **112**: 3293–302.
50 Sze DM, Giesajtis G, Brown RD *et al.* Clonal cytotoxic T cells are expanded in myeloma and reside in the CD8(+)CD57(+)CD28(−) compartment. *Blood* 2001; **98**: 2817–27.
51 Champagne P, Ogg GS, King AS *et al.* Skewed maturation of memory HIV-specific CD8 T lymphocytes. *Nature* 2001; **410**: 106–11.
52 Bandres E, Merino J, Vazquez B *et al.* The increase of IFN-gamma production through aging correlates with the expanded CD8(+high)CD28(−) CD57(+) subpopulation. *Clin Immunol* 2000; **96**: 230–5.
53 Brenchley JM, Karandikar NJ, Betts MR *et al.* Expression of CD57 defines replicative senescence and antigen-induced apoptotic death of CD8+ T cells. *Blood* 2003; **101**: 2711–20.
54 Bleul CC, Fuhlbrigge RC, Casasnovas JM, Aiuti A, Springer TA. A highly efficacious lymphocyte chemoattractant, stromal cell-derived factor 1 (SDF-1). *J Exp Med* 1996; **184**: 1101–9.
55 Peled A, Grabovsky V, Habler L *et al.* The chemokine SDF-1 stimulates integrin-mediated arrest of CD34(+) cells on vascular endothelium under shear flow. *J Clin Invest* 1999; **104**: 1199–211.
56 Brouty-Boye D, Doucet C, Clay D, Le Bousse-Kerdiles MC, Lampidis TJ, Azzarone B. Phenotypic diversity in human fibroblasts from myelometaplasic and non-myelometaplasic hematopoietic tissues. *Int J Cancer* 1998; **76**: 767–73.

doi: 10.1111/j.1349-7006.2009.01468.x

Prognostic significance of CUB domain containing protein expression in endometrioid adenocarcinoma

SUHANA MAMAT[1,3], JUN-ICHIRO IKEDA[1], TAKAYUKI ENOMOTO[2], YUTAKA UEDA[2], NUR RAHADIANI[1], TIAN TIAN[1], YI WANG[1], YING QIU[1], TADASHI KIMURA[2], KATSUYUKI AOZASA[1] and EIICHI MORII[1]

Departments of [1]Pathology and [2]Obstetrics and Gynecology, Osaka University Graduate School of Medicine, Yamada-oka 2-2, Suita 565-0871, Japan; [3]Department of Basic Health Science, Kulliyyah of Allied Health Sciences, International Islamic University Malaysia, 25200 Kuantan, Pahang, Malaysia

Received December 10, 2009; Accepted February 2, 2010

DOI: 10.3892/or_00000753

Abstract. CDCP1, a transmembrane protein with intracellular tyrosine residues which are phosphorylated upon activation, is supposed to be engaged in proliferative activities and resistance to apoptosis of cancer cells. High level of CDCP1 expression proved to be a poor prognosticator for lung adenocarcinoma. Here, expression level of CDCP1 was immunohistochemically examined in 110 cases (median age of 54.7 years) of endometrioid adenocarcinoma, and its clinical implications were evaluated. Tumor stage was stage I in 71 cases (64.5%), II in 5 (4.5%), III in 28 (25.5%), and IV in 6 (5.5%). Staining intensity of tumor cells was divided into two categories; tumor cells with no to weak and moderate to strong membrane staining. The intensity of CDCP1 expression in each case was defined by the staining of major population of cells as follows; cases with tumor cells showing no to weak and moderate to high membrane staining were categorized as CDCP1-low and CDCP1-high, respectively. Eighty-seven of 110 cases were categorized as CDCP1-high, and the remaining as CDCP1-low. Significant positive correlation was observed between low CDCP1 expression and stage (p=0.0091), relapse rate (p=0.0017), and poor prognosis (p=0.0009). Multivariate analysis revealed that low CDCP1 and advanced stage were independent poor prognostic factors for both OS and DFS. As compared to cancer cells, normal endometrium continuously expressed CDCP1. These suggested that the attitude of CDCP1 in cancers of lung and endometrium was different. Different role of CDCP1 by tissues and cancers is discussed.

Introduction

CDCP1 is originally identified as an epithelial tumor antigen expressed in the lung cancer cell lines but not in normal lung tissues (1). CDCP1 is a transmembrane protein with three extracellular CUB domains, which are important for cell-cell interactions, and intracellular tyrosine residues, which are phosphorylated upon activation (1-4). Physiologically, CDCP1 expression is limited to stem or progenitor cells in the hematopoietic and mesenchymal tissues, and no significant expression has been reported in developed tissues (5,6). CDCP1 protects cells from anoikis, a form of apoptosis triggered by loss of cell survival signals generated from interaction of cells with extracellular matrix (7).

We previously reported the epigenetic regulation of CDCP1 expression in the cell lines derived from various malignancies, such as leukemia and colon adenocarcinoma, and in the clinical samples of breast cancer (8,9). CDCP1 expression level is correlated with proliferative activities of tumor cells in breast cancer (8). Uekita *et al* reported that the knocked-down expression of CDCP1 in lung adenocarcinoma cell line by RNA interference abolishes *in vitro* colony formation and *in vivo* metastatic abilities (7). Among cases with lung adenocarcinoma, high CDCP1 expression proved to be an independent factor for poor prognosis of patients (10). Recent study revealed CDCP1 expression to be an independent negative prognostic factor for renal cell carcinoma (11). These findings indicate that CDCP1 plays an important role in tumorigenesis and metastasis, and that the high level of CDCP1 expression suggests aggressiveness of malignancies.

Endometrioid adenocarcinoma is the most common invasive malignancy of the female genital system (12,13). Despite the advances in the methods for detection and treatment, prognosis of patients with endometrioid adenocarcinoma still remains unfavorable. In the present study, CDCP1 expression was immunohistochemically examined in clinical samples with endometrioid adenocarcinoma, and its clinical implications were evaluated.

Materials and methods

Patients and methods. One hundred and ten patients who underwent surgery for endometrioid adenocarcinoma at Osaka University Hospital during the period from January 1998 to January 2007 were examined. Clinicopathological findings in

Correspondence to: Dr Eiichi Morii, Department of Pathology, Graduate School of Medicine, Osaka University, Yamada-oka 2-2, Suita 565-0871, Japan
E-mail: morii@patho.med.osaka-u.ac.jp

Key words: CDCP1, endometrioid adenocarcinoma, prognosis, immunohistochemistry, normal endometrium

Table I. Summary of characteristics in 110 endometrioid adenocarcinoma patients.

	No. of patients
Tumor	
T1	79
T2	10
T3	20
Stage	
I	71
II	5
III	28
IV	6
Tumor histological grade	
1	44
2	43
3	23
Menopausal status	
Premenopausal	
Postmenopausal	
Estrogen receptor status	
Positive	75
Negative	35
Progesterone receptor status	
Positive	66
Negative	44
Recurrence	
Positive	22
Negative	87
Prognosis	
Deceased	15
Alive (with recurrence)	8
Alive (with no recurrence)	87

these 110 patients are summarized in Table I. There were 110 women with ages ranging from 22 to 75 (median, 54.7 years). Resected specimens were macroscopically examined to determine the location and size of the tumors. Normal (3 cases of proliferative and 4 of secretory phases), atrophic (3 cases), and hyperplastic endometrium (6 cases), together with endometrial polyp (2 cases), obtained from patients with functional bleeding, were included as control tissues. Histologic specimens were fixed in 10% formalin and routinely processed for paraffin-embedding. Paraffin-embedded specimens were stored in the dark room in the Department of Pathology of Osaka University Hospital at room temperature, sectioned at 4 μm thickness at the time of staining, and stained with hematoxylin and eosin and immunoperoxidase procedure. The histological stage was determined according to the International Federation of Obstetricians and Gynecologists (FIGO) staging system (14). All patients were followed up with laboratory examinations including routine peripheral blood cell counts at 1-6-month intervals, roentgenogram, computed tomographic scan and pelvic examination at 6-12-month intervals. The follow-up period for survivors ranged from 7 to 122 (median, 82) months. The study was approved by the ethics review board of Graduate School of Medicine, Osaka University.

Immunohistochemistry for CDCP1, estrogen receptor (ER), progesterone receptor (PgR) and MIB-1. CDCP1 expression was immunohistochemically examined with use of anti-CDCP1 antibody (Abcam Ltd., Cambridge, UK). The proliferative activity of cancer cells was examined with monoclonal antibody MIB-1 (Immunotech, Marseilles, France), recognizing the proliferation-associated antigen Ki-67. Expression status of ER and PgR was estimated with anti-ER (Dako) and anti-PgR (Dako) antibodies, respectively. After antigen retrieval with Pascal pressurised heating chamber (Dako A/S, Glostrup, Denmark), the sections were incubated with anti-CDCP1, anti-ER, anti-PgR antibody and MIB-1, diluted at x200, x2, x6 and x100, respectively. Then, the sections were treated with biotin-conjugated anti-goat IgG (Zymed, South San Francisco, CA, USA) for CDCP1 staining, or with biotin-conjugated anti-mouse IgG (Dako A/S) for ER, PgR and MIB-1 staining. After washing, the sections were incubated with the peroxidase-conjugated biotin-avidin complex (Vectastain ABC kit, Vector, Burlingame, CA). DAB (Vector) was used as a chromogen. As the negative control, staining was carried out in the absence of primary antibody. Stained sections were evaluated independently by two pathologists (J.I. and E.M.) based on the manner described previously (10). Briefly, staining intensity of tumor cells was divided into two categories; tumor cells with no to faint and moderate to strong membrane staining. The intensity of CDCP1 expression in each case was defined by the staining of major population of cells as follows; cases with tumor cells showing no to faint staining were categorized as CDCP1-low, and those showing moderate to strong membrane staining as CDCP1-high. Proportion and intensity of ER and PgR expression were evaluated as described by Allred *et al* (15). The MIB-1 labeling index was defined as the percentage of stained nuclei per 1000 cells. The cases were divided into MIB-1-high and MIB-1-low groups using the median as cut-off value.

RNA extraction and quantification of CDCP1 mRNA level by real-time reverse transcription (RT)-PCR. RNA was extracted from paraffin sections using an RNeasy FFPE kit (Qiagen, Valencia, CA). Total RNA was subjected to reverse transcription by Superscript III (Invitrogen, Carlsbad, CA), and the single strand cDNA was obtained. The mRNA levels for CDCP1 and GAPDH genes were verified using TaqMan gene expression assays (Applied Biosystems, Foster City, CA) as recommended by the manufacturer. The amount of CDCP1 mRNA was normalized to that of GAPDH mRNA, and the normalized value was shown as relative mRNA amount.

Statistical analysis. Statistical analyses were performed using StatView software (SAS Institute Inc., Cary, NC). The χ^2 and Fisher's exact probability test were used to analyze the

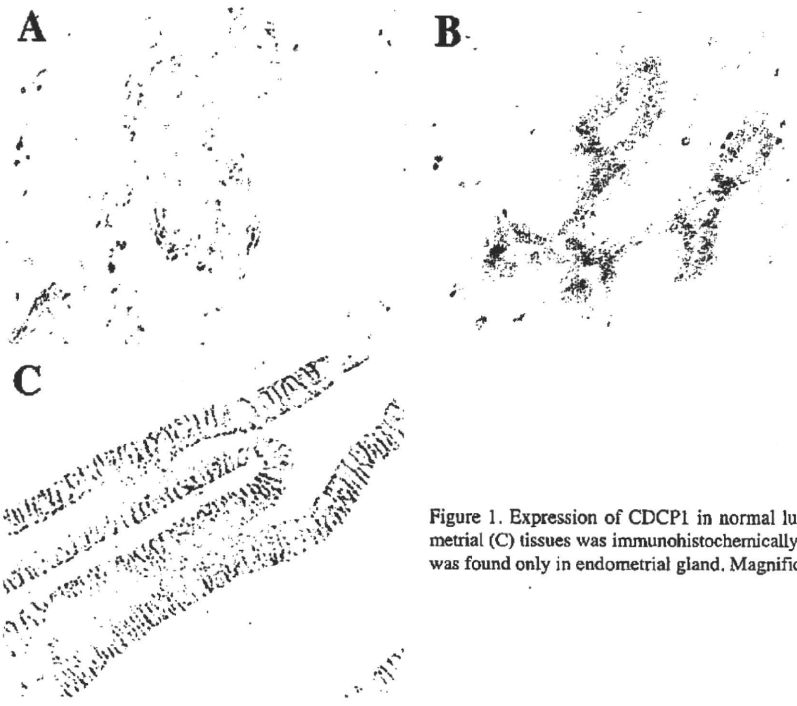

Figure 1. Expression of CDCP1 in normal lung (A), breast (B), and endometrial (C) tissues was immunohistochemically examined. CDCP1 expression was found only in endometrial gland. Magnification, x400.

Table II. Correlation between CDCP1 expression and MIB-1 index in normal and non-cancerous endometrium.

	CDCP1 expression		
	Low	High	P-value
MIB-1 labeling index			
≥20	4	12	
<20%	2	0	0.0339

correlation between CDCP1 expression and clinicopathological factors in endometrioid adenocarcinoma. Kaplan-Meier methods were used to calculate overall survival (OS) and disease-free survival (DFS) rate, and differences in survival curves were evaluated with the log-rank test. Cox's proportional hazards regression model with a stepwise manner was used to analyze the independent prognostic factors. The p-values <0.05 were considered to be statistically significant.

Results

Immunohistochemical findings. Our previous study on lung and breast carcinomas revealed that CDCP1 expression was hardly detected in adjacent normal tissues (Fig. 1A and B) (9). Whereas high level of CDCP1 expression was found not only in endometrioid adenocarcinoma cells but also in adjacent normal endometrium (Fig. 1C). Then, CDCP1 expression was examined in normal (proliferative and secretory phases, Fig. 2A and B), atrophic (Fig. 2C), and hyperplastic endometrium (Fig. 2D), together with endometrial polyp (Fig. 2E). Strong CDCP1 expression was detected in all examined endometrial tissues, although the expression level was slightly lower in atrophic and secretory phase endometrium. The MIB-1 labeling index correlated with the CDCP1 expression level in the non-neoplastic endometrial glands (Table II).

Next, the expression of CDCP1 was examined in 110 endometrioid adenocarcinoma tissues. Staining intensity of tumor cells was divided into two categories; tumor cells with no to faint, and moderate to strong, membrane staining (Fig. 3). Eighty-seven (79.1%) of 110 cases were categorized as CDCP1-high, and the remaining as CDCP1-low.

Correlation of intensity in immunohistochemical staining with level of CDCP1 mRNA expression. RNAs were extracted from the endometrioid adenocarcinomas immunohistochemically showing CDCP1-high and CDCP1-low expression, and normal endometium (each three cases). Level of CDCP1 mRNA expression was higher in CDCP1-high adenocarcinoma and normal endometrium than in CDCP1-low cases (Fig. 4). Level of CDCP1 expression in CDCP1-high adenocarcinoma was comparable to that of normal endometrium.

Correlation of CDCP1 expression with clinical variables. Correlation of CDCP1 expression with clinicopathological features was evaluated. Significant positive correlation was observed between CDCP1-low expression and relapse rate (p=0.0017), stage (p=0.0091), poor prognosis (p=0.0009), and tumor grade (p=0.0108). Other parameters including tumor size, Ki-67 index, ER and PgR did not correlate with CDCP1 expression (Table III). Tumor stage in the present patients was stage I in 71 cases (64.5%), II in 5 (4.5%), III in 28 (25.5%), and IV in 6 cases (5.5%). The 5-year DFS and OS were 86.7%

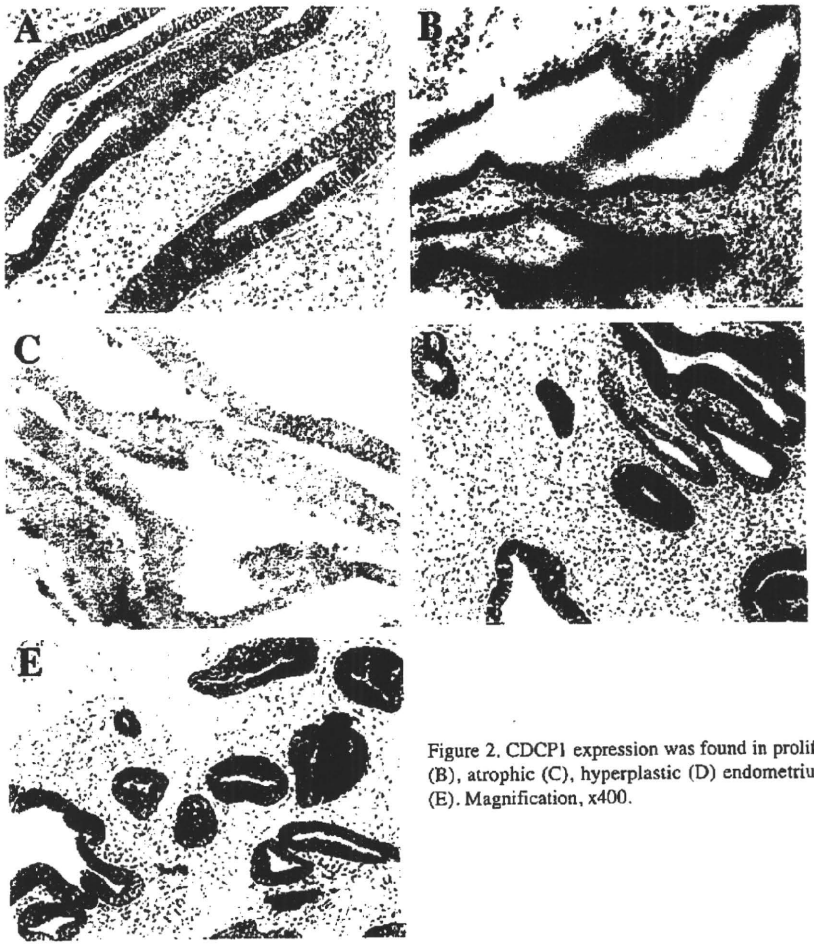

Figure 2. CDCP1 expression was found in proliferative (A), secretory phase (B), atrophic (C), hyperplastic (D) endometrium, and endometrial polyps (E). Magnification, x400.

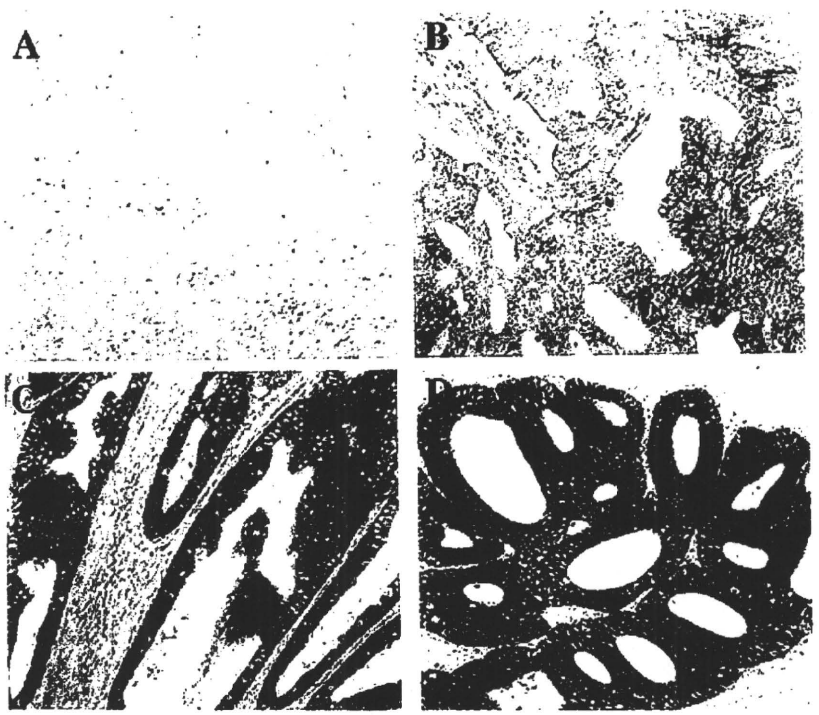

Figure 3. Staining of CDCP1 in endometrioid adenocarcinoma. Representative fields of CDCP1-low (A and B) and -high (C and D) cases are shown. Magnification, x400.

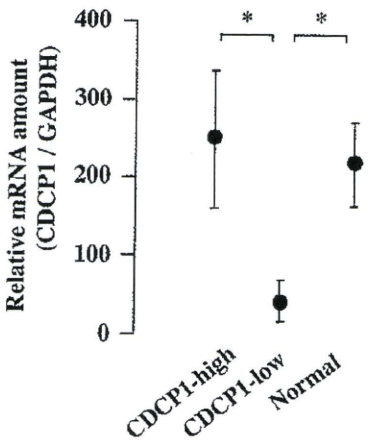

Figure 4. Correlation of CDCP1 expression at mRNA and protein level. RNAs were obtained from CDCP1-high and CDCP1-low endometrioid adenocarcinoma, and normal endometrium. The values represent the mean ± SE of three cases. *p<0.05 by the Student's t-test.

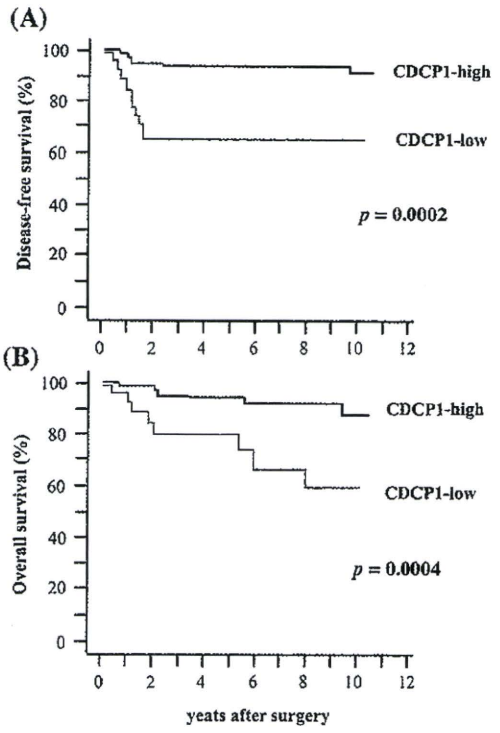

Figure 5. Kaplan-Meier plots. Survival curves of disease-free (A) and overall (B) are shown. CDCP1-low cases showed less favorable disease-free and overall survival.

and 90.6%, respectively. Tumors recurred in 22 patients. Of these, 15 patients died of their tumors. There was a statistically significant difference in DFS rates (p=0.0002) and OS rates (p=0.0004) between patients with CDCP1-high and CDCP1-low tumors (Fig. 5).

Univariate analysis showed that stage, tumor grade, and CDCP1 expression were significant factors for both OS and DFS (Table IV). The multivariate analysis revealed that CDCP1 expression and stage were independent prognostic factors for both OS and DFS (Table IV); the patients with CDCP1-low expression showed a less favorable prognosis than those with the high expression.

Table III. Correlation between CDCP1 expression and clinicopathological parameters.

	CDCP1 expression		
	Low	High	P-value
Tumor			
T1	13	66	
T2	4	6	
T3	6	14	0.0718
Stage			
I	10	61	
II	0	5	
III	12	16	
IV	1	5	0.0091
Tumor histological grade			
1	6	38	
2	7	36	
3	10	13	0.0108
Estrogen receptor status			
Positive	16	64	
Negative	8	23	0.5375
Progesterone receptor status			
Positive	15	64	
Negative	8	23	0.4288
MIB-1 labeling index			
≥20	9	37	
<20%	13	50	0.8907
Recurrence			
Positive	10	12	
Negative	13	74	0.0017
Prognosis			
Deceased	8	7	
Alive (with recurrence)	2	6	
Alive (with no recurrence)	13	74	0.0032

Discussion

The characteristics of patients, such as age and stage, in the current study were similar to those in a previous report, indicating that the results obtained from the current study are commonly applicable to endometrioid adenocarcinoma worldwide (16). Our previous data on lung adenocarcinoma showed that the high level of CDCP1 expression in the tumor cells was a factor of poor prognosis (10). As in the cases of lung adenocarcinoma, CDCP1-high expression is a negative prognosticator in breast and renal cancers (8,11). In the